COMPUTATIONAL APPROACH FOR AUTOPHAGY AND APOPTOSIS SPECIFC KNOWLEDGEBASES-GUIDED SYSTEM PHARMACOLOGY DRUG RESEARCH

By

Nanyi Wang

Bachelor of Science, Sichuan University, 2015

Submitted to the Graduate Faculty of

School of Pharmacy in partial fulfillment

Of the requirements of the degree of

Master of Science

University of Pittsburgh

2017

UNIVERSITY OF PITTSBURGH

SCHOOL OF PHARMACY

This thesis was presented

By

Nanyi Wang

It was defended on

March 28th, 2017

and approved by

Dandan Sun, MD, PhD, Professor

Xiang-Qun (Sean) Xie, PhD, Professor

Lirong Wang, PhD, Research Assistant Professor

Dissertation Advisor: Xiang-Qun (Sean) Xie, PhD., Professor

COMPUTATIONAL APPROACH FOR AUTOPHAGY AND APOPTOSIS SPECIFC KNOWLEDGEBASES-GUIDED SYSTEM PHARMACOLOGY DRUG RESEARCH

Nanyi Wang, MS

University of Pittsburgh, 2017

Autophagy and Apoptosis are the basic physiological processes in cells to clean up aged and mutant cellular components or even the entire cells. However, both autophagy and apoptosis are disrupted in most of the major diseases like cancer and neurological disorder. Increasing attention is also paid recently in academia to understand the crosstalk between autophagy and apoptosis due to their tight synergetic or opposite functions in several pathological processes. To assist autophagy and apoptosis related drug research, we established two chemical-genomic databases which are specifically designed for autophagy and apoptosis, by collecting protein targets, chemicals, and pathways closely related to autophagy and apoptosis. This information, supported by our established system pharmacological analysis tools, such as HTDocking and TargetHunter, provided two comprehensive knowledgebases for the pharmacological study of autophagy and apoptosis. Additionally, to enhance the accuracy of the prediction by HTDocking in these two knowledgebases, we developed ProSeletion, a computational protein selection algorithm bases on the research purpose, is designed to generate the proper structure subset for molecular docking study. A suggested docking score threshold for active ligands (SDA) was then generated according to the receiver operating characteristic (ROC) curve and was used as an individual docking score criterion for the active ligands prediction. The performance of

prediction was further evaluated by FDA recently approved small molecule antineoplastic drugs. Overall, the Autophagy Knowledgebase and the Apoptosis Knowledgebase will accelerate our work in autophagy-apoptosis related research and can be a useful tool for information searching, target prediction, and new chemical discovery.

Key words: Autophagy; Apoptosis; Cancer; Neurological disease.

TABLE OF CONTENTS

LIST OF TABLES

LIST OF FIGURES

PREFACE

I'm deeply thankful to my advisor Dr. Xiang-Qun (Sean) Xie for his guidance and support for my research during the past two years. I would also thank Dr. Lirong Wang for his kind encouragement, suggestions and powerful technical support for my thesis. And Dr. Zhiwei Feng helped me a lot while conducting the molecular docking part in this thesis. Thank all of our group members for their help and guidance. Their suggestions in each group meeting are very informative and valuable. Thank all the committee members, Dr. Xiang-Qun (Sean) Xie, Dr. Lirong Wang and Dr. Dandan Sun for the valuable suggestions. The fund for this project is provided by NIDA (P30 DA035778A1) from Xiang-Qun (Sean) Xie's lab.

Doing research is always interesting but challenging. I particularly enjoy the days while finding and solving new problems. I wish all our members and friends will pursue successful careers in the future no matter in the academia or the industry.

1. INTRODUNCTION

1.1 Autophagy

Autophagy is a process by which cells capture intracellular lipids, proteins, and organelles, and transport them into lysosomes for degradation[1]. It is also known as a lysosomal degradative pathway with the character of the formation of double-membrane autophagic vesicles (AV), also named autophagosomes. When lysosome fuses with the outer membrane of the AV, a degradation will happen to the AV inner membrane as well as the contents inside[2, 3]. Three different autophagic pathways are reported: (1) macroautophagy, (2) mitophagy, and (3) chaperone-mediated autophagy (CMA)[4]. Among them, macroautophagy is the most common autophagic pathway in the eukaryotic cell in which lysosomes directly engulf part of the cytoplasm for further degradation (Figure 1).

Autophagy occurs at low basal levels in almost all cells with the homeostatic functions such as protein and organelle turnover[1]. This prevents the gradual accumulation of proteins and organelles overtime. However, autophagy is dramatically upregulated when intracellular energy and nutrients are required by cells in certain conditions, for instance, during starvation, protein aggregation, organelles damage, growth factor withdrawal or in a high bioenergetics demand status. This allows the stability of synthetic pathways and energy homeostasis in cells.

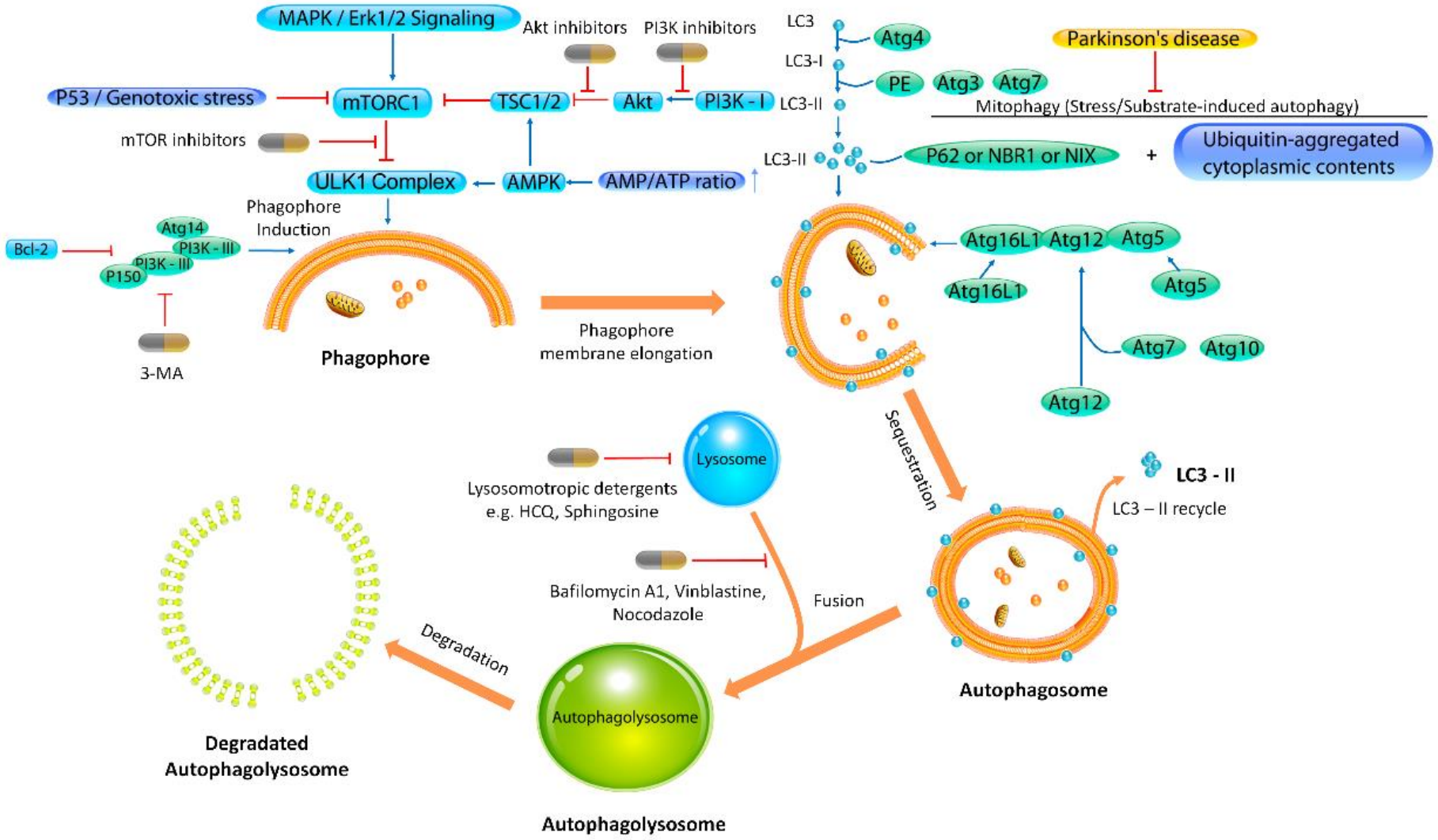
MAPK / Erk1/2 Signaling
Akt inhibitors
PI3K inhibitors
LC3
LC3-I
LC3-II
Atg4
PE
Atg3
Atg7
Parkinson's disease
Mitophagy (Stress/Substrate-induced autophagy)
P53 / Genotoxic stress
mTORC1
TSC1/2
Akt
PI3K - I
mTOR inhibitors
ULK1 Complex
AMPK
AMP/ATP ratio
P62 or NBR1 or NIX
+
Ubiquitin-aggregated cytoplasmic contents
Phagophore Induction
Bcl-2
Atg14
PI3K - III
P150
3-MA
Phagophore
Phagophore membrane elongation
Atg16L1
Atg12
Atg5
Atg7
Atg10
Sequestration
Lysosome
Lysosomotropic detergents e.g. HCQ, Sphingosine
LC3 - II
LC3 – II recycle
Bafilomycin A1, Vinblastine, Nocodazole
Fusion
Autophagosome
Degradation
Autophagolysosome
Degradated Autophagolysosome
Autophagolysosome

Figure 1. Autophagy process and signaling through macroautophagy

Macroautophagy is the most common subtype of autophagy. It starts from the phagophore induction to autophagolysosome formation then degradation. Autophagy related genes (ATGs) involved autophagy is majorly regulated through mTOR. Most of the autophagic-related genetics and kinase signaling are involved in this process before the formation of autophagosome while the stability of lysosome and autophagosome is the major determinant for this process after autophagosome formation.

The capability of autophagy to capture, degrade, eliminate and recycle intracellular components affects metabolism, enables host defense, regulates trafficking, remodels the proteome, alters signaling and influences cellular interactions[5]. This makes the intracellular homeostasis possible and enables the normal cells functional in almost every cell.

1.2 Autophagy and diseases

1.2.1 Autophagy and cancer

1.2.1.1 Autophagy inhibits cancer initiation

Autophagy is believed to have an important role in cancer development. Over past decades, studies of how autophagy impacts cancer development indicate a link between carcinogenesis and decreased levels of autophagy[6].

Comparison of normal and autophagy-defective mice and cells has revealed the suppressive role of autophagy in cancer development. Mice with autophagy defects accumulate abnormal mitochondria, autophagy adaptor p62, and ubiquitinated keratin[7-9].

Although the functional consequences on protein and organelle of this dysfunction are not completely clear, they are associated with reactive oxygen species (ROS) production, activation of the DNA damage response, cell damage, and death. This will further lead to a chronic inflammatory state due to the failure of autophagy-mediated cellular garbage disposal[10, 11]. Chronic tissue damage and inflammation are associated with DNA-damaging ROS production, contributing to mutations that can initiate cancer and promote tumor progression[12].

Although the mechanisms by which autophagy functions in cancer suppression remain unclear, in the field of cancer initialization, autophagy is more likely to be an inhibitor rather than a promoter of initial oncogenesis.

1.2.1.2 Autophagy promotes cancer survival

Although autophagy is suppressed during the early stage of cancer initiation, it apparently has a role in the enhancement of cancer cell survival within the cancer microenvironment and will be upregulated during the later stages of cancer progression as a cytoprotective mechanism against the stressful conditions. Autophagy maintains the survival of both normal cells and cancer cells and is stimulated in vivo by cellular stress, including nutrient, growth factor, and oxygen deprivation[10, 13, 14]. When in vitro models take stress into consideration, the contribution of autophagy to cell survival becomes clearer. For instance, autophagy-defective cancer cells undergoing metabolic stress showed impaired survival in comparison with autophagy-proficient cells[15]. Therefore, an upregulated autophagy in response to stress in cancer cells is still important for survival due to the high-stressed microenvironment around them. In a search based on NextBio to investigate the effects of

FDA approved oncology drugs on autophagy pathways (Aug 2016), most the anticancer drugs are accompanied by an upregulation on autophagy related signaling pathways (Table 1). Yasuko also raised a similar conclusion that autophagy is activated in cancer cells in response to various anticancer therapies[16], including Tamoxifen treatment, Temozolomide treatment, Rapamycin treatment, sodium butyrate and SAHA treatment, andγ-irradiation. This further supports the notion that an increasing level of autophagy occurs as a response to intracellular stress.

Table 1. Modulation of autophagy by 134 anticancer drugs

Category	Direction	Ratio	Percentage
Overall	up	95/134	71%
	down	39/134	29%
Chemotherapy	up	41/53	77%
	down	12/53	23%
Hormonal therapy	up	11/14	79%
	down	3/14	21%
Immunotherapy	up	1/2	50%
	down	1/2	50%
Other	up	18/28	64%
	down	10/28	36%
Unknown Mechanism	up	25/38	66%
	down	13/38	34%

Autophagy served as an energy recycler for cancer cells and is one of the mechanisms which promote the survival of the drug-resistant cancer cells[17]. Under harsh conditions, nutrients are recycled and provided again for the cancer cells and the cellular stress is reduced because of the autophagy[17]. In several preclinical studies, autophagy significantly reduces the

efficacy of different anticancer agents in various categories including vorinostat, imatinib and cyclophosphamide[18].

In general, autophagy has dual roles during tumorigenesis. It limits genomic damage and suppresses tumor initiation on one hand while helping cancer cells to survive during stress on the other hand. Because of the dual roles of autophagy, the single-agent using of inhibitor can results in different outcomes[18] due to the functional existence of both damage cleaning and autophagic cell death (ACD). Therefore, further study is needed before autophagic modulators can be clinically used, based on its context-dependent nature.

1.2.1.3 Target autophagy for therapy in cancer

Since autophagy is a cancer survival pathway in most cases and the basal level of autophagy is significantly increased in several cancer cells, a great interest in inhibiting autophagy is raised in cancer therapy. By inhibiting autophagy, cancer cells may suffer from more serious stress caused by an increasing amount of cellular waste and energy crisis. The drug-resistant cancer cells can be sensitized again to anticancer therapy by autophagy inhibition[19]. For instance, hydroxychloroquine (HCQ), a lysosomotropic detergent, which blocks the degradation of autophagosome by inhibiting lysosome function, is recently being actively investigated in the clinic[15]. Although whether HCQ will be able to effectively block autophagy in human cancer is not yet resolved, a trend of developing autophagy inhibitors for cancer combination therapy is already underway. Either targeting on the latter stage like lysosome fusion with autophagosome or earlier signaling in phagophore and autophagosome formation is promising. Besides later autophagic stage drugs like HCQ, several small

molecule inhibitors of PI3K/AKT/MTOR pathway which target at the earlier stage are also under clinical investigations (Table 2). However, the signaling feedback of PI3K/AKT/MTOR inhibition, like FOXO-dependent feedback and ERK amplification, can cause several negative effects[20]. Thus, development of more potent and selective (cell selective and autophagic stage selective) autophagy inhibitors and drug combinations are in high demand both in academia and industry.

Table 2. Summary of autophagy related small-molecule drugs in clinical research

Target	Drug	Mechanism	Autophagy modulation	Phase	Ref
Autophagosome formation					
PI3K/AKT/mTOR pathway	Sirolimus (Rapamycin)	mTOR inhibitor	Induce	4	21
	Curcumin	mTOR inhibitor	Induce	3	22
	Resveratrol	mTOR inhibitor	induce	3	23
	AZD8055	mTOR inhibitor	Induce	1	24
	Dactolisib	PI3K and mTOR inhibitor	Induce	2	25
	BGT226	PI3K and mTOR inhibitor	Induce	2	26
	Voxtalisib	PI3K and mTOR inhibitor	Induce	2	27
	SF1126	PI3K and mTOR inhibitor	Induce	1	28
	Pilaralisib	PI3K inhibitor	Induce	2	29
	Sonolisib	PI3K inhibitor	Induce	2	30
	Pictilisib	PI3K inhibitor	Induce	1	31
	Buparlisib	PI3K inhibitor	Induce	3	32
	Idelalisib	PI3K inhibitor	Induce	4	33
	Perifosine	AKT inhibitor.	induce	3	34
	GSK690693	AKT inhibitor	Induce	1	35
	Triciribine phosphate	AKT inhibitor	Induce	2	36
	MK2206	AKT inhibitor	Induce	2	37
AMPK activation	Metformin	Cause AMPK activation, inhibition mTOR pathway	Induce	4	38
	Trehalose	Chemical chaperone, Induce AMPK activation	induce	2	39

	Rilmenidine	Induce AMPK activation.	induce	4	40
Lysosomal function					
Lysosome membrane stability	Chloroquine	Endosomal Acidification Inhibitor, TLR signaling inhibitor, Lysosomal lumen alkalizer	Inhibit	4	41
	Hydroxychloroquine	Lysosomal lumen alkalizer. Blocks the fusion of the autophagosome and lysosome	Inhibit	4	42
	Pantoprazole	proton pump inhibitor (PPI)	Inhibit	4	43
Selective autophagy					
HDAC	Vorinostat	HDAC1, HDAC2 and HDAC3 (Class I) and HDAC6 (Class II) inhibitor	Induce	4	44
Sirtuin-1	Resveratrol	Activates sirtuin-1, inhibits P70 S6 kinase, induce AMPK activation	Induce	3	45
Other					
Hormonal	Tamoxifen	Antiestrogens. Target at oestrogen receptor and cause accumulation of Sterols	Induce	4	46
Ca2+–calpain–GSα pathways	Verapamil	L-type Ca^{2+} channel blocker, reduce intracytosolic Ca2+ levels.	Induce	4	47
Phosphoinositol signaling pathway	Carbamazepine	MIP synthase inhibitor. Reduce inositol and IP3 Levels	Induce	4	48
cAMP–Epac–PLC-ε–IP3 pathway	Clonidine	Imidazoline-1 receptor agonists. Reduce cAMP levels.	induce	4	49

1.2.1.3.1 Drugs targeting PI3K/AKT/MTOR pathway

The PI3K-AKT signaling pathway is inappropriately activated in many cancers. Several genetic abnormalities are known to activate this signaling including the loss of PTEN tumor suppressor and the somatic mutations of class I_A PI3K such as E542K, E545D, and E545K[50]. The activation of PI3K-AKT signaling will induce the formation of mammalian target of rapamycin complex 1 (mTORC1) and further enhance the phagophore formation in the autophagy initiation (Figure 1). Numerous drugs are designed for this pathway and some of them are already in the clinical trials (Table 2). Among these inhibitors for PI3K/AKT/MTOR pathway, Sirolimus (rapamycin) is recognized as the first-in-class mTORC1 inhibitor which binds to the mTORC1 allosteric site[51]. However, further studies have observed that mTOR catalytic-site inhibitors were more potent than Sirolimus. Catalytic-site inhibitors, like AZD8055 (IC_{50} = 0.8 nM against mTOR), have minimal effect on the phosphorylation site of several AKT substrates despite a strong effect on AKT S473 phosphorylation (mTORC2 inhibition)[52]. This effect is more closely related to the complete mTORC1 inhibition rather than the phosphorylation of AKT.

1.2.1.3.2 Drugs targeting AMPK activity

As a metabolic sensor, AMP-activated protein kinase (AMPK) regulates glucose, lipid and cholesterol metabolism and is closely related with cell metabolism[17]. Activation of the AMPK pathway by an increasing ratio of AMP/ATP inhibits the mTOR signaling on serine/threonine kinase ULK1 (ULK1) complex and would then induce the autophagy initiation (Figure 1). This happens through the stimulation of cAMP-inositol 1,4,5-trisphosphate (IP3) or calpain-G-stimulatory protein α (Gsα) pathways[47]. AMPK is

believed to have a major upstream regulator serine/threonine kinase LKB1 (STK11). However, other regulators are still available such as calcium, calmodulin-dependent protein kinase kinase 2 (CAMKK2) and transforming growth factor-β-activating kinase 1 (TAK1)[17]. Several drugs like metformin and rilmenidine can regulate the phagophore formation via this pathway (Table 2).

1.2.1.3.3 Drugs targeting lysosome membrane

Stability of the lysosome membrane is critical for lysosomal function and its ability to fuse with the autophagosome (Figure 1). Elevated lysosomal pH has been linked to autophagy failure and neurological disorders[53]. Several drugs such as chloroquine (CQ) and hydroxychloroquine (CQ) can disrupt the lysosome membrane and therefore inhibit the autolysosome formation (Table 2). An impairment of autophagic vesicle clearance can also be observed due to the CQ accumulation. Based on the data from clinical trials acquired from clinicaltrials.gov, CQ and HCQ have been used in more than half of the autophagy-related clinical research. This may due to their relatively powerful inhibition of autophagy because of the mechanism of the late-stage autophagy inhibition. Compared to CQ, HCQ was found having fewer side effects partly because of its hydrophilic property and disability to cross the blood brain barrier (BBB)[54].

1.2.1.3.4 Drugs targeting on other autophagy related pathways

Several other pathways can also regulate the autophagy process (Table 2). By inhibiting the members of histone deacetylases (HDAC) or activating the sirtuin-1, drugs are able to induce the signaling for selective autophagy. Hormonal, Ca^{2+}–calpain–GSα, Phosphoinositol, and cAMP–Epac–PLC-ε–IP3 pathways are also been demonstrated to influence the

autophagy process.

1.2.2 Autophagy and neurological diseases

1.2.2.1 Autophagy in neurological diseases

Autophagy is essential in maintaining the brain homeostasis[55]. With aging process, neuronal cells will accumulate abnormal intracellular proteins and damaged organelles just like other cells. However, as a post-mitosis cell type, neurons cannot dilute cellular waste by mitosis. Thus, autophagy is more necessary for neurons to get rid of toxic aggregate-prone proteins[56]. This reliance was also demonstrated by the severe functional affection in primary lysosomal disorders or lysosomal-related gene mutations. One of the shared pathological features of most adult-onset human neurodegenerative diseases is the formation of intracytoplasmic aggregates within neurons and other cell types[4]. This is observed by many researchers in the field of Alzheimer's disease (where tau and Aβ accumulate in cytoplasm) and Parkinson disease (where α-synuclein aggregates in Lewy Bodies). A common approach of studying these neurological diseases is to investigate whether autophagy is involved in the accumulation of aggregate-prone and mutant proteins. Hara and Komatsu reported that instead of being relatively inactive, basal autophagy is relatively active in neurons for the clearance of abnormal proteins in cytoplasm[11, 57]. This is crucial for inhibiting the pathological protein aggregation in the cytoplasm, even in the absence of disease-related mutations. However, both macroautophagy and chaperone-mediated autophagy (CMA) are significantly less efficient during aging process[58]. Therefore, autophagy failure is one of the most popular concepts in explaining the disease mechanism. When we consider when and

where the autophagy halts, the autophagy induction, cargo sequestration, selective autophagy and autophagosome clearance (lysosome digestion) are the major steps where the dysfunctions may occur[59]. Collectively, these studies implicate a normal, relatively active autophagy is needed in brain and any disruption in physiological autophagy may lead to abnormal protein behavior, for instance, aggregation or oligomerization.

Increased function of autophagy is relatively common in neurodegenerative disease as a response to mutant, damaged proteins or defective autophagy itself[59]. A search among 148 central nervous system agents based on NextBio database shows 82% of these agents are associated with an increased autophagy (Table 3). Although induction of autophagy is generally regarded as neuroprotective, this induction in some acute injuries like hypoxic ischemic brain injury may be overexuberant[60], in which the cellular stress for autophagy is excessively induced. Therapeutic plans in such situation are complex. However, in certain disease in which the function of autophagy is not known being substantially compromised, for instance, Huntington's disease, an induction in autophagy might be a beneficial strategy.

Table 3. Modulation of autophagy by 148 central nervous system (CNS) agents

Category	Direction	Ratio	Percentage
CNS Agents	up	122/148	82%
	down	26/148	18%

1.2.2.2 Deficient autophagy in Alzheimer's disease

Alzheimer's disease (AD) is a neurodegenerative disorder characterized by progressive dementia and brain morphological changes such as atrophy, senile plaques with fibrillogenic beta amyloid (Aβ), and intraneuronal neurofibrillary tangles (NFT) with hyperphosphorylated tau[4]. In AD, macroautophagy (referred as autophagy in most cases), the major subtype of autophagy, is considered to be most relevant to AD[61]. In 2005, Nixon's group identified immature autophagic vacuoles (AVs) accumulation in dystrophic neuritis in AD brains using immunogold labeling and electron microscopy[62]. However, proper formation and degradation of autophagosome are important for maintaining a normal autophagic function. In hippocampus neurons of AD mice, abnormal accumulation of immature AVs in axon has also been reported even before the neuronal and synaptic loss[63]. This indicates a malfunctioned autophagy is accompanied with AD. As reported by Wolfe, AD is associated with an awry lysosomal digestion and a possible PSEN1 or ApoE4 mutation which may lead to a deficiency in vATPase, Rab5 or Rab7 activation, and substrate overload in lysosomes[64]. Other factors contributing to AD include but not limit to ApoE4[65], reactive oxygen species (ROS), accumulated Aβ peptides, tau oligomers, oxidized lipids and lipoproteins that disrupt lysosomal proteolysis. However, dysfunction of autophagy is whether the cause or the result of AD is still in debate. The difference in many factors including animal models and cellular models may lead to controversies. For β-amyloid, autophagy plays a critical role in the clearance of Aβ by facilitating the degradation of amyloid precursor protein (APP) as well as APP cleavage products including Aβ[66, 67]. However, Yu reported that Aβ can also be produced in immature autophagic vacuoles in AD brains[68]. In the case of tau protein,

autophagy-lysosome system dysfunction will lead to the formation of insoluble aggregates and tau oligomers, while enhancing of autophagy can restrict this aggregation[69]. As a conclusion, deficient autophagy is likely to be a player in the AD progression brain with an inhibited lysosomal proteolysis function.

1.2.2.3 Autophagy dysfunction in Parkinson disease

In Parkinson disease (PD), accumulation of α-synuclein within Lewy bodies (LBs) in the aubstantia nigra is sufficient to cause death of dopaminergic neurons and PD[70]. Autophagic vacuoles accumulate when α-synuclein is overexpressed in mutant or even wild-type transgenic mice[71]. Although α-synuclein can be degraded by the proteasome, α-synuclein itself is a substrate for autophagy[72] and is preferentially degraded by autophagy system. Moreover, α-synuclein was demonstrated to inhibit autophagy at a very early stage when over-expressed[73]. Besides α-synuclein, PD-related gene products such as parkin, DJ-1, PINK1, and LRRK2 are also found in LBs which number far exceeds their normal presence in brain[74]. Among these, Leucine-rich repeat kinase 2 (LRRK2) mutation involves in the most common autosomal-dominant form of PD. Change in LRRK2 activity as a result of PD-related mutations was associated with defected endosomal-lysosomal trafficking, lysosomal pH, chaperone-mediate autophagy, and calcium regulation[59]. Finding of the specific inhibitors for LRRK2 encoded kinase has been a potential therapeutic direction of research. Generally, autophagy dysfunction, including several autophagy-related mutations, mislocations or duplications of important PD-related genes and proteins contribute to the Parkinson's disease.

1.2.2.4 Target autophagy for therapy in neurodegeneration

Autophagy is a promising but challenging target for neurological therapies due to its powerful but delicate nature. Identification of specific autophagic stage(s) interrupted in different neurological diseases is crucial for future stage-targeted drug development. Available evidence prefers autophagy inducing strategies that specifically targeting the autophagic stages that are significantly disrupted in each disease. For enhancing autophagy induction and sequestration (beginning stage), administration of rapamycin, a relatively selective inhibitor of mTORC1, restricts the degeneration of neurons in transgenic mouse models of Huntington's disease[75], Alzheimer's disease[76], Parkinson's disease[72] and Prion disease[21]. Trehalose, possibly through AMPK activation, promotes the clearance of mutant huntingtin, tau, and α-synuclein while showing neuroprotective effects both in cell and transgenic mouse model[77]. A combination of compounds with AMPK and mTOR activity may also have additive benefits[78]. For selective autophagy enhancement, histone deacetylase inhibitors may increase the mutant huntingtin acetylation and selectively targets it to autophagosomes which is known to be beneficial in Huntington's disease models[79]. Enhancing lysosome efficiency and stability are also possible strategies for autophagy targeting therapy in neurodegeneration. However, most of the approaches in this field are at a genetic level while few drugs are available.

Although the autophagy enhancement is more preferred, activation of autophagy can cause damage in the neurodegenerative diseases where a massive accumulation of undegraded immature autophagic vacuoles (AVs) was present. In this situation, treatments that inhibit autophagosome formation shows an improvement, at least temporarily, in neuronal viability[80]. Although no compounds are yet available, the optimal treatment in these

cases should enhance the autophagosome clearance instead of inducing more which remains undegraded.

1.3 Apoptosis

Apoptosis is also known as programmed cell death. Morphological changes during apoptosis include both the cytoplasm and nucleus alterations which are interestingly similar across species and cell types. In the nucleus, the chromatin condenses and breaks while the ribosomes and mitochondria in cytoplasm aggregates. The fragments of dead apoptotic cells form a structure named "apoptotic bodies". Generally, three major changes take place during apoptosis: 1) caspases activation 2) protein and DNA breakdown 3) membrane changes and being recognized by phagocytic cells[81]. Among them, caspases are crucial in the apoptotic signaling since they are both the initiators and executioners. Three pathways are known to activate caspases in which two are frequently described, intrinsic and extrinsic pathways of apoptosis. In the extrinsic pathway, binding of death ligands (FAS ligands, TNFα or TRAIL) to death receptors coupled with FADD will consequently activate caspase-8 and finally the apoptosis. While in the intrinsic pathway where the mitochondria have an important role, cytotoxic damages will deliver signals to mitochondria and initiates the apoptosis (Figure 2). Although extrinsic apoptosis is efficient enough to activate caspase-3 and kill the cells, intrinsic apoptosis can be activated by caspase-8 in the extrinsic pathway which will amplify the death signal.

Apoptosis is understood as a stress induced process of cellular communication[82]. It is more likely to occur under the conditions of cellular stress like genetic damage or severe

oxidative stress which are relatively common in several diseases (like cancer) and their therapies. Therefore, apoptosis is always taken into consideration in disease and drug research as one of the disease mechanisms or therapeutic targets.

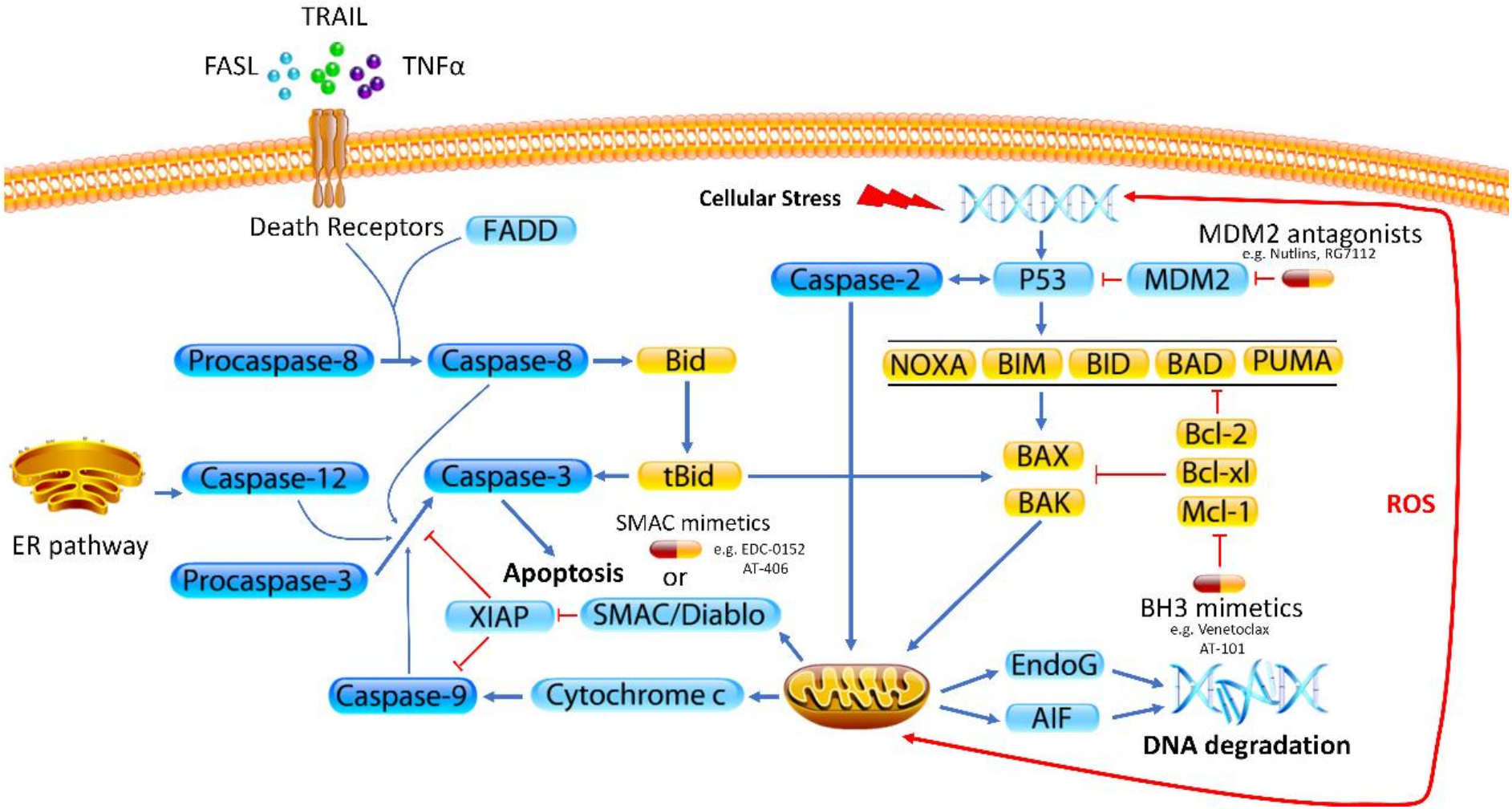
TRAIL
FASL
TNFα
Death Receptors
FADD
Cellular Stress
MDM2 antagonists
e.g. Nutlins, RG7112
Caspase-2
P53
MDM2
Procaspase-8
Caspase-8
Bid
NOXA
BIM
BID
BAD
PUMA
Bcl-2
Bcl-xl
Mcl-1
BAX
BAK
Caspase-12
Caspase-3
tBid
ER pathway
SMAC mimetics
e.g. EDC-0152
AT-406
Procaspase-3
Apoptosis
or
XIAP
SMAC/Diablo
BH3 mimetics
e.g. Venetoclax
AT-101
ROS
EndoG
AIF
Caspase-9
Cytochrome c
DNA degradation

Figure 2. Apoptosis signaling

Apoptotic pathways are generally categorized into three types. In the extrinsic pathway, different types of death receptors can be activated by either FAS ligand, TNFα or TRAIL followed by a formation of DISC complex (TRAIL and FAS ligand) or signaling complex 1 (TNFα). Consequently, the procaspase-8 and -10 cleavages will occur which results in caspase-8 and -10 activation. Caspase-8 and -10 will then amplify the death signal either by directly activating effector caspases or enhancing Bid binding to BAX and BAK which will lead to intrinsic pathway activation. In the intrinsic pathway, cellular stress can either directly activate BAX and BAK or transcriptionally upregulate BAX and BAK through p53.

1.4 Apoptosis and diseases

1.4.1 Apoptosis and cancer

The ability to evade apoptosis is one of the hallmarks of cancer. Evasion of apoptosis may benefit the tumor development, progression and even resistance to treatment. Cancer cells utilize a variety of mechanisms to evade apoptosis, and some are specific to certain cancer types while others are not. Generally, this evasion is supported by: 1) either increased level of antiapoptotic molecules or decreased level of proapoptotic molecules[83]; 2) reduced signaling of death receptor; and 3) impaired caspase function. For the pro-apoptotic and anti-apoptotic proteins balance disruption, Bcl-2 family of proteins, p53 and inhibitor of apoptosis proteins (IAPS) are popularly discussed as the major contributors[81]. For death receptors, receptors downregulation, functional impairment or level changes in death receptor ligands are believed to impact apoptotic extrinsic pathway. For reduced caspase function,

downregulation in caspase proteins is always considered as a major issue. As a conclusion, any of these changes listed above in cancer cells can altering the apoptotic function. However, the major contributor in each case is still largely dependent on the situation and the type of cancer.

1.4.2 Target apoptosis pathways in cancer therapy

Targeting apoptosis pathways in cancer therapeutic has been a promising direction during the past few decades. Based on a recent search (May 2016) on the NexiBio database, most of the anticancer drugs now in the market can induce apoptosis (Table 4). While most of these molecules enhance the autophagic function indirectly, few of them are designed to induce autophagy directly. In the recent few years, increasing number of drugs which directly target apoptosis pathways have entered clinical trials. The importance of several drug targets has also been demonstrated. This includes but not limited to the Bcl-2 family of proteins, p53, surviving, IAP and caspases. One drug (Venetocalx), which targets on Bcl2, has already been approved by the FDA in April 2016 (Table 5).

Table 4. Modulation of apoptosis by 149 anticancer drugs.

Category	Direction	Ratio	Percentage
Overall	up	90/149	60%
	down	59/149	40%
Chemotherapy	up	43/61	70%
	down	18/61	30%
Hormonal therapy	up	11/14	79%
	down	3/14	21%
Immunotherapy	up	4/4	100%
	down	0/4	0%
Other	up	11/28	39%
	down	17/28	61%
Unknown Mechanism	up	24/42	57%
	down	18/42	43%

1.4.2.1 Drugs targeting Bcl-2 family proteins

Bcl-2 family proteins are in tight balance in cells, either decreased expression of pro-apoptotic Bcl-2 members or overexpression of anti-apoptotic Bcl-2 members can inhibit capase-9 activation, which is the major pathway for intrinsic apoptosis activation. Bcl-2 family overactivation has been observed in several tumors including lymphocytic leukemia (CLL) where the application of Bcl-2 agents may be more promising. Drugs like ABT-263 (Table 5) targeting at Bcl-2/Bcl-w/Bcl-xl may lead to thrombocytopenia. This is due to the inhibition of Bcl-xl which is important in platelet survival[84]. Drugs which are more Bcl-2 selective, such as Venetocalx, are much preferable for apoptotic Bcl-2 targeting. Particularly, MAO-B inhibitors, like Rasagiline, regulate the autophagy via the downstream bcl-2 pathway.

Table 5. Summary of apoptosis related small-molecule drugs in clinical research

Target	Drug	Mechanism	Direction	Phase	Ref
Bcl-2 family of proteins					
BH3 mimetics	Venetoclax (ABT-199)	Bcl-2 selective inhibitor	Induce	4	85
	Navitoclax (ABT-263)	Bcl-2, Bcl-xL, Bcl-w inhibitor	Induce	2	86
	Obatoclax	Pan Bcl-2 inhibitor that binds to Bcl-2, Bcl-xL, Bcl-w, Bcl-B, BFL-1 and Mcl-1	Induce	3	87
	(-)-Gossypol	Pan Bcl-2 inhibitor. Affinity for Bcl-2, Bcl-xL and Mcl-1 at submicromolar concentrations.	Induce	2	88
MAO-B inhibitors	Rasagiline	Selective and irreversible inhibitor of MAO-B. Activate protein kinase C and down regulating FAS and Bax family of proteins	Inhibit	4	89
	Selegiline	Selective inhibitor of MAO-B. Up-regulating Bcl-2 protein	Inhibit	4	89
SMAC mimetics					
Targeting both XIAP and cIAPs	GDC-0152	IIAPs antagonist. Binds to the BIR3 domain of XIAP, cIAP1 and cIAP2	Induce	1	90
	CUDC-427	IAPs antagonist	Induce	1	91
	Birinapant	IAPs antagonist	Induce	2	92
	LCL161	IAPs antagonist	Induce	2	93
	AT-406	IAPs antagonist.	Induce	1	94
Targeting p53-MDM2	RG7112	Inhibit MDM2-p53 interaction	Induce	1	95
	CGM-097	Inhibit MDM2-p53 interaction	Induce	1	96
Other	Minocycline	Prevents release of cytochrome c. Increase Bcl-2 expression and inhibit the activity of caspase-1 and -2	Inhibit	4	97

1.4.2.2 Drugs targeting IAPS

Inhibitor of apoptosis proteins (IAPs) are attractive molecular targets for cancer therapy, which also has various abilities in blocking apoptosis. So far, one member in the IAPs, XIAP, has drawn much attention due to its directly binding with caspase-3, -7 and -9 and the inhibition of the caspase activity. Both the intrinsic and extrinsic pathways (Figure 2) can be effectively inhibited by XIAP. Although several second mitochondria-derived activator of caspases (SMAC) mimetics such as IAPs antagonists GDC-0152 and Birinapant have entered clinical trials, none of them has yet been approved. Almost all the SMAC mimetics may induce a TNFα-mediated toxicity. This makes the development of IAPS targeting cancer therapy more challenging.

1.4.2.3 Drugs targeting p53

P53 is important in transcriptional regulation and signaling. Several small-molecule inhibitors of MDM2-p53 interaction, such as Nutlins and MI-219[84] have been developed as the lead compounds which show some inhibition of tumor growth in vivo. More MDM2 targeting chemicals are then synthesized while some enter the clinical trials (Table 5). Other potential therapies based on p53 can be grouped into gene therapy and immunotherapy. However, in p53 gene therapy, although a few studies once went into Phase III, none was finally approved.

1.4.3 Apoptosis and Neurological Disease

1.4.3.1 Apoptosis in Neurological Diseases

Apoptosis is important in neuron development. It controls the type and number of different neuron cells in the developing brain and spinal cord[98]. However, under certain

pathologic conditions like the aged brain, apoptosis is also co-responsible for neuron loss. The individual neuron may die rapidly when the apoptosis is fully activated and this further accelerates the progression of neurodegeneration.

1.4.3.2 Apoptosis in Alzheimer's disease

Although the exact mechanisms of neuronal degeneration in AD are still unknown, available data supports that the accumulation of Aβ peptide will lead to ROS generation and induce apoptosis[99], especially when an unfunctional autophagy is present where the Aβ cannot be cleared properly. In another experiment, when exposed to Aβ, apoptosis in cultured neurons was induced directly which made cells more vulnerable to death-induced conditions like increased oxidative stress and reduced energy[100]. Death receptor 4 (DR4) and 5 (DR5) were shown to mediate the Aβ induced apoptosis in cerebral microvascular endothelial cells and primary culture of astrocytes[98]. Aggregation of APP in mitochondria due to the overexpression of Aβ will activate caspase-3 and then initiate the apoptosis process. Beside Aβ peptide, other factors like RanBP9, presenilin-1/-2 and ER calcium release have also shown contributions in the apoptosis under AD.

1.4.3.3 Apoptosis in Parkinson's disease

Apoptosis is thought to be the dominant mechanism for neurodegeneration in PD[101]. Several proteins that signal for apoptosis are changed during PD. This includes the increasing of proapoptotic effector BAX, decreasing of Beclin-1 and the mutation of DJ-1 and Parkin encoded by PARK2 gene. However, generally, the exact mechanism of apoptosis in PD pathogenesis is still not clear.

1.4.3.4 Target apoptosis for therapy in neurodegeneration

Most of the drug developing strategy for neurodegeneration diseases is focusing on drugs that inhibit neuronal dysfunction or early death in the disease progression. In the aspect of molecular signaling, the strategy for treating neurodegeneration is completely the opposite compared to strategies in cancer treatment. Here, blocking the apoptotic triggers or inducing the anti-apoptotic proteins is clearly a better option, although the protein targets, like Bcl-2, BAX or caspase, remain the same compared to apoptotic cancer therapy. Minocycline, an antibiotic which inhibits apoptosis by disrupting caspase-3 activation and preventing ROS, also increases the Bcl-2 expression, is demonstrated to prevent the aggravation of several neurodegeneration diseases in animal models[98]. The similar beneficial effect was also observed on other apoptosis related drugs like CEP-1347 (inhibitor of MLK) and Rasagiline (MAO-B inhibitor).

1.5 Crosstalk between autophagy and apoptosis

1.5.1 Functional level

The relationship between autophagy and apoptosis at functional level can be divided into three categories (Figure 3). Both autophagy and apoptosis can induce cell death directly. However, autophagy can also either inhibit or induce apoptosis under different cellular conditions.

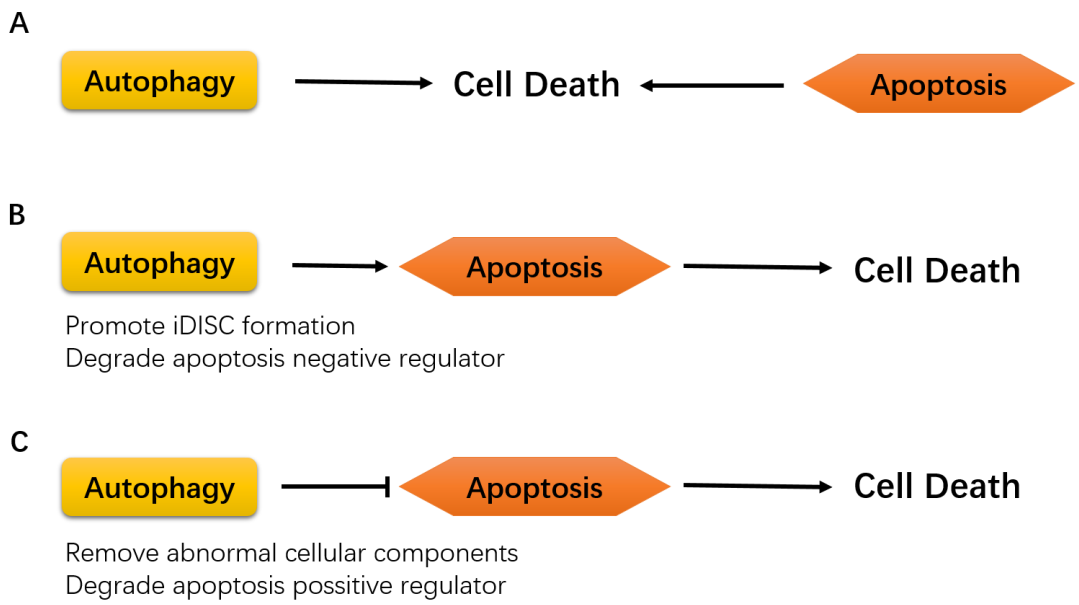

Figure 3. Autophagy and apoptosis relationship at functional level.

(A) Both autophagy and apoptosis is sufficient to induce cell death. (B) Autophagy can promote apoptosis induced cell death by promoting death-inducing signaling complexes (iDISC) or enhancing the apoptosis negative regulators degradation. (C) Autophagy can also inhibit apoptosis induced cell death by degradation of apoptosis positive regulators such as PUMA or by removal of damaged organelles and protein aggregates.

1.5.2 Signaling level

Apoptosis is interacted with autophagy in both its intrinsic and extrinsic pathway. Mitochondrial outer membrane permeabilization (MOMP) is important in apoptosis intrinsic pathway since it controls the release of mitochondrial intermembrane proteins including the cytochrome c which will lead to caspase-9 activation. Bcl-2 family proteins control MOMP. Anti-apoptotic proteins Bcl-2, Bcl-X and Mcl-1 prevent the activation of pro-apoptotic proteins Bax and Bak under basal cellular conditions[102]. In the aspect of autophagy, BCL

family proteins also participate in the phagophore formation (Figure 1). The crosstalk between autophagy and intrinsic apoptosis pathway happens tightly around BCL-2 family proteins (Figure 4). In extrinsic pathway, death ligands such as TRAIL have a significant role. However, autophagy deficient cells are highly sensitive to TRAIL induced apoptosis[102]. This is due to the regulatory effect of autophagy on PUMA, a protein which regulate the MOMP. Therefore, autophagy and apoptosis are not exclusive processes. They act either synergistically or antagonistically to maintain the homeostasis in cells. However, this balance is always disrupted during disease progression. Generally, autophagy is considered as one of the cell survival mechanisms during cancer chemotherapeutics due to its attempt of removing damaged cellular components[18]. It may further lead to the inhibition of apoptosis induced cell death. While apoptosis is a cell death mechanisms when comparing to autophagy.

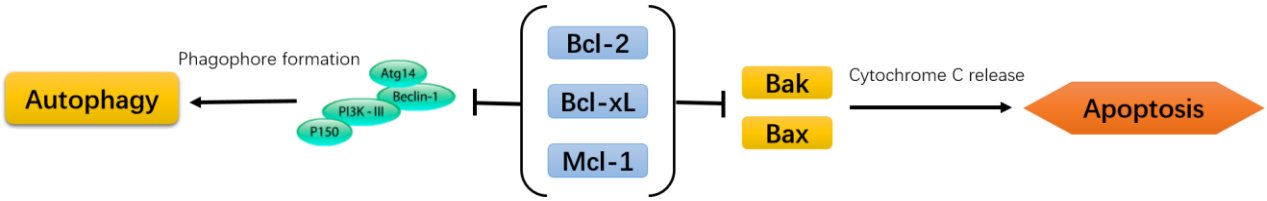

Figure 4. Bcl-2 family proteins in the cross talk

Anti-apoptotic Bcl-2 family proteins (Bcl-2, Bcl-xL and Mcl-1) inhibit both the autophagy and apoptosis initiation.

2. METHOD AND MATERIAL

2.1 Autophagy and apoptosis knowledgebases construction

2.1.1 Knowledgebases infrastructure and web interface

The autophagy (http://www.cbligand.org/autophagy) and apoptosis ((http://www.cbligand.org/apoptosis) knowledgebases were established based on the chemogenomics database AlzPlatform (www.CBLIgand.org/AD) which was previously constructed by Dr. Xiang-Qun Xie's group[103], with an apache (http://www.apache.org/) web server and a MySQL (http://www.mysql.com) database. Openbabel (http://openbabel.org/) was integrated in the knowledgebases as the search engine for chemical structures. Autodock (http://autodock.scripps.edu/) was used as the docking engine for target-prediction with several our in house chemoinformatics tools, for instance, BBB Predictor and HTDocking[104], implemented. The web interface is written in PHP language (http://www.php.net/).

2.1.2 Data sources

2.1.2.1 Proteins and compounds library

Autophagy and apoptosis related proteins and compounds were collected from literatures and public databases, including PubMed (www.ncbi.nlm.nih.gov/pubmed), PubChem (pubchem.ncbi.nlm.nih.gov/), Metacore (https://portal.genego.com/), DrugBank (http://www.drugbank.ca), SciFinder (https://scifinder.cas.org/), UniProt (http://www.uniprot.org/) and CHEMBL (https://www.ebi.ac.uk/chembl/). Totally, 201 and 456 candidate protein targets were collected for autophagy and apoptosis respectively. The targets corresponding X-ray crystallographic structures were acquired directly from RSCB

Protein Data Bank (www.rcsb.org/pdb) to construct the protein library for autophagy and apoptosis.

2.1.2.2 Pathways and Bioassays

Signaling pathways for autophagy and apoptosis are acquired from public databases including Metacore (https://portal.genego.com/), KEGG (http://www.genome.jp/kegg/), and DrugBank (https://www.drugbank.ca/) and was revised based on published literatures. The associated bioassays for the target proteins, which were used to statistically validate our prediction, were collected from literatures and the public databases mentioned above.

2.1.2.3 System pharmacological analysis tools

HTDocking. High-throughput docking (HTDocking) is an internet-based computing tool that automatically conducts docking procedure to explore the compound-protein interactions (http://www.cbligand.org/AD/docking_search.php). In the autophagy and apoptosis knowledgebases, crystal structures of proteins related to autophagy or apoptosis are collected from the RSCB Protein Data Bank (PDB) to build two domain-specific subsets: autophagy specific and apoptosis specific. AutoDock Vina is set as the docking engine at the backstage[105]. Co-crystallized ligands and water molecules were removed from the original PDB structure and hydrogen atoms were added. The active binding pocket of individual proteins was defined by the residues near the cocrystallized ligands (generally known inhibitors) or generated by the AutoDock utility scripts. Three to five predicted binding affinity values (ΔG values) of different docking poses for each compound in a binding pocket of a protein can be provided by AutoDock Vina. Docking scores in the HTDocking program were generated based on the best binding affinity value. The docking score is calculated as

pKi, where pKi = -log(predicted Ki) and the predicted Ki = exp(ΔG×1000/(1.9871917×298.15). The docking score of a queried compound from each protein structure is used to assess and rank the potential protein partners or targets.

TargetHunter. TargetHunter is a ligand-based chemical genomics tool (http://www.cbligand.org/TargetHunter) which was designed based on the concept that compounds which are structurally similar have great possibility sharing similar targets and biological profiles[106]. By using the TAMOSIC Algorithm and the MCM Algorithm, TargetHunter can provide not only the targets information but also structures of the similar compounds and their associated bioassays for any input compounds.

Blood–Brain Barrier (BBB) Predictor. Blood–brain barrier (BBB) is the single most critical factor restricting the neurotherapeutic agents. Since both autophagy and apoptosis have important roles in neurodegeneration diseases, the BBB predictor (http://www.cbligand.org/BBB/) was particularly designed to distinguishing whether a drug-like molecule can cross the BBB or not. This predictor was established by a combination of LiCABEDS[107] algorithms and support vector machine (SVM)[108] and on four types of fingerprints of 1593 reported compounds[109].

2.2 Protein structure subset generation

For each of the individual protein target in autophagy and apoptosis databases, more than one crystal structures are usually available on RSCB Protein Data Bank (Table 6). By using the ProSelection, a computational protein selection algorithm designed to generate the structure subset in which protein structures of "weak selector" were filtered out while

structures of "strong selector" were kept base on the docking protocol and research purpose. Either two independent samples t-test or nonparametric Mann-Whitney U test with Bonferroni correction was applied in this research to select the protein structure subsets for the protein targets in the autophagy and apoptosis knowledgebases. Choosing of the statistical method was determined by the normality of docking score distribution. Specifically, two independent samples t-test[110] will be used only if the docking scores are normally distributed in both active and inactive ligands set. Otherwise, the Mann-Whitney U test[111] will be used to calculate the p value due to the required normality assumption of t-test. All statistical tests in this research are one-tailed. A widely used open source python package Scipy[112] (https://www.scipy.org/) is used to conduct the statistical analysis in this research.

In the statistical selection of PDB structures in autophagy and apoptosis knowledgebases, active and inactive ligands for each protein targets are collected from CHEMBL database and stored into two independent groups. Active ligands are defined as molecules with an IC_{50} lower than 500 nM while the inactive ligands have an IC_{50} higher than 50 μM. Molecular weight for active and inactive ligands are set between 200 – 800 Da to get proper docking results in Molecular Docking[113]. Active and inactive ligands were docked to their associated protein targets and the docking scores were returned. Statistical tests were then applied to the docking scores to investigate the mean difference of docking scores between active ligands and inactive ligands against each protein targets, respectively.

Table 6. Number of available crystal structures for the 19 protein targets

(data collected from RSCB Protein Data Bank in Aug 2016)

Protein name	Method	Number of crystal structures
ABL1_HUMAN	X-ray	53
PIM2_HUMAN	X-ray	2
MTOR_HUMAN	X-ray	16
AKT3_HUMAN	X-ray	1
AKT2_HUMAN	X-ray	16
AKT1_HUMAN	X-ray	22
PK3CA_HUMAN	X-ray	19
SIR2_HUMAN	X-ray	20
SIR1_HUMAN	X-ray	8
LRRK2_HUMAN	X-ray	2
INSR_HUMAN	X-ray	29
HDAC6_HUMAN	X-ray	8
CATM_HUMAN	X-ray	3
CATD_HUMAN	X-ray	6
CATB_HUMAN	X-ray	11
CASP1_HUMAN	X-ray	29
B2CL1_HUMAN	X-ray	48
BCL2_HUMAN	X-ray	11
PDPK1_HUMAN	X-ray	67

Abbreviations: PDPK1, 3-phosphoinositide-dependent protein kinase 1; B2CL1, Bcl-2-like protein 1; CASP1, Caspase-1; CATB, Cathepsin B; CATD, Cathepsin D; HDAC6, Histone deacetylase 6; INSR, Insulin receptor; SIR1, NAD-dependent protein deacetylase sirtuin-1; SIR2, NAD-dependent protein deacetylase sirtuin-2; PK3CA, Phosphatidylinositol 4,5-bisphosphate 3-kinase catalytic subunit alpha isoform; AKT1, RAC-alpha serine/threonine-protein kinase; AKT2, RAC-beta serine/threonine-protein kinase; MTOR, Serine/threonine-protein kinase mTOR; ABL1, Tyrosine-protein kinase ABL1.

2.2.1 Test of Normality

The normality of docking score distributions is determined based on D'Agostino and Pearson's test which combines skew and kurtosis to produce an omnibus test of normality[114, 115] (function name in Python: scipy.stats.mstats.normaltest). Protein structures which have normal-distributed docking scores in both its own active and inactive ligand sets will be selected to run the two independent sample t-test with unequal variance at 95% significance level. Structures which have non-normal distributed docking scores against either of the ligand sets will be chosen for Mann-Whitney U test at 95% significance level.

2.2.2 Two independent samples t-test

The t-Test for two independent samples[110] is a statistical test used to measure the mean difference between two groups of data. Data in both groups need to be normally distributed. The general equation of the t-Test for two independent samples is shown below:

$$t = \frac{\bar{x}_1 - \bar{x}_2}{\sqrt{\frac{s_1^2}{n_1} + \frac{s_2^2}{n_2}}}$$

If $t \leq 0$, then $p = 2\times(area\ to\ the\ left\ of\ t\ under\ a\ t_{d''}\ distribution)$

If $t \geq 0$, then $p = 2\times(area\ to\ the\ right\ of\ t\ under\ a\ t_{d''}\ distribution)$

Where d'' is the nearest integer to the approximate degrees of freedom, $\bar{x}_1$ and $\bar{x}_2$ are the averages of docking scores for active ligands and inactive ligands, respectively. Ligand numbers in each ligand set are represented by n_1 and n_2. Variance of the two input samples is referred as s_1^2 and s_2^2.

Then the exact p-value can be computed by

$$p = 2\times[1 - \Phi(T)]$$

2.2.3 Mann-Whitney U test

The Mann-Whitney U test[111] (also named Wilconxon Rank-Sum Test) is a nonparametric analog to the t test for two independent samples. This test can be used only when each of the two independent samples has a sample size larger than 10. This equals to the minimum number of valid active/inactive ligands required for running the statistical selection. The general equation in Mann-Whitney U test is shown below:

If $R_1 \neq n_1(n_1 + n_2 + 1)/2$ and there are no ties, then

$$T = \left[\left|R_1 - \frac{n_1(n_1 + n_2 + 1)}{2}\right| - \frac{1}{2}\right] \Big/ \sqrt{\left(\frac{n_1 n_2}{12}\right)(n_1 + n_2 + 1)}$$

If $R_1 \neq n_1(n_1 + n_2 + 1)/2$ and there are ties, then

$$T = \left[\left|R_1 - \frac{n_1(n_1 + n_2 + 1)}{2}\right| - \frac{1}{2}\right] \Big/ \sqrt{\left(\frac{n_1 n_2}{12}\right)\left(n_1 + n_2 + 1 - \frac{\sum_{i=1}^{g} t_i(t_i^2 - 1)}{(n_1 + n_2)(n_1 + n_2 - 1)}\right)}$$

If $R_1 = n_1(n_1 + n_2 + 1)/2$, then T = 0.

Where R_1 refers to the rank sum in the first sample, t_i refers to the number of observations with the same value in the ith tied group, and g is the number of tied groups.

Then the exact p-value can be computed by

$$p = 2\times[1 - \Phi(T)]$$

2.2.4 Bonferroni correction

Correction for multiple comparison needs to be applied to the Mann-Whitney U test above because of the existence of multiple PDB structures for each protein target. Bonferroni correction[116] was chosen due to its commonly usage, in which the significance level α is adjusted to $\frac{\alpha}{m}$, where m is the number of hypothesis tests. The equation used for converting Mann-Whitney U test or two independent samples t-test p value to Bonferroni corrected p value is shown below:

$$(1 - p)^k = 1 - p_0$$

Where p refers to the original p value, p_0 is the Bonferroni corrected p value, k is the number of PDB structures for certain target.

Crystal structures with a Bonferroni corrected p value larger than 0.05 will be considered as "weak selector" due to their incapability of distinguishing its active ligands from inactive ligands base on the selected docking protocol. In the opposite, structures which can significantly distinguish active ligands from inactive ligands ($p < 0.05$) will be labeled as "strong selector".

Particularly, most of the structures for kinases in this research are labeled based on their

ability of distinguishing ATP competitive inhibitors due to the docking pocket we used. This indicates that the "weak selector" may not be a bad crystal structure if taking other docking pockets or other research purpose into consideration.

2.3 Individual docking score criteria

Interpreting the docking results is an important issue when molecular docking is conducted on a bunch of protein targets and their associate chemical ligands. We raised a hypothesis that the docking score distributions are different among different protein structures of protein targets. This indicates that the docking score criterion for active ligands may be specific for each individual target. A Suggested docking score threshold for active ligands (SDA) is used in this research as an individual docking score criterion.

SDA is generated based on the receiver operating characteristic (ROC) curves[117]. The ROC curve is established by stepping sequentially through the ranked list of test-set compounds arranged in order of increasing docking scores for each target. True positive rate (TPR) and false positive rate (FPR) are calculated at each ranking score. Plotting the TPR versus FPR for all positions in the ranked list will generate the ROC plot. One interesting feature of the ROC curve is the capability of generating the optimized cutoff point. In this work, cutoff point is calculated for each ROC curve to guarantee at least one correct prediction in the top 3 predictions (also means not all of the top 3 predictions are wrong, quantitatively, $FPR^3 \leq 0.0001$) before minimizing the distance between top-left point in the ROC plot and selected points on the ROC. The final optimized cutoff points were reported and their associated docking scores are recorded as SDA. Any ligand that has a docking score

higher than corresponding SDA will be considered as an “active” ligand against its associated crystal structure.

2.4 Validation Compound Set Establishment.

Compound set for testing the performance of the “strong selector” structures is generated from the FDA-approved small molecule antineoplastic drugs since 2005 (www.fda.gov). The molecular weight is set as from 200 Da to 800 Da and 43 qualified compounds were included in the validation compound set.

3. RESULTS

3.1 Autophagy related protein targets and drugs

Autophagy knowledgebase (www.cbligand.org/autophagy) archived 102 autophagy related protein targets, 32 autophagy related FDA-approved and clinical trial drugs, 10,971 target-associated chemicals, 137 related signaling pathways, 16,209 bioactivity records, and 13,326 references.

3.2 Apoptosis related protein targets and drugs

Apoptosis knowledgebase (www.cbligand.org/apoptosis) archived 455 autophagy related protein targets, 14 autophagy related FDA-approved and clinical trial drugs, 24,357 target-associated chemicals, 96 related signaling pathways, 12,756 bioactivity records, and 89,039 references.

3.3 Targets overlap between autophagy and apoptosis

Totally 455 and 102 protein targets are summarized in the Apoptosis Knowledgebase and Autophagy Knowledgebase, respectively. Among these targets, 37 targets are overlapped (Figure 5).

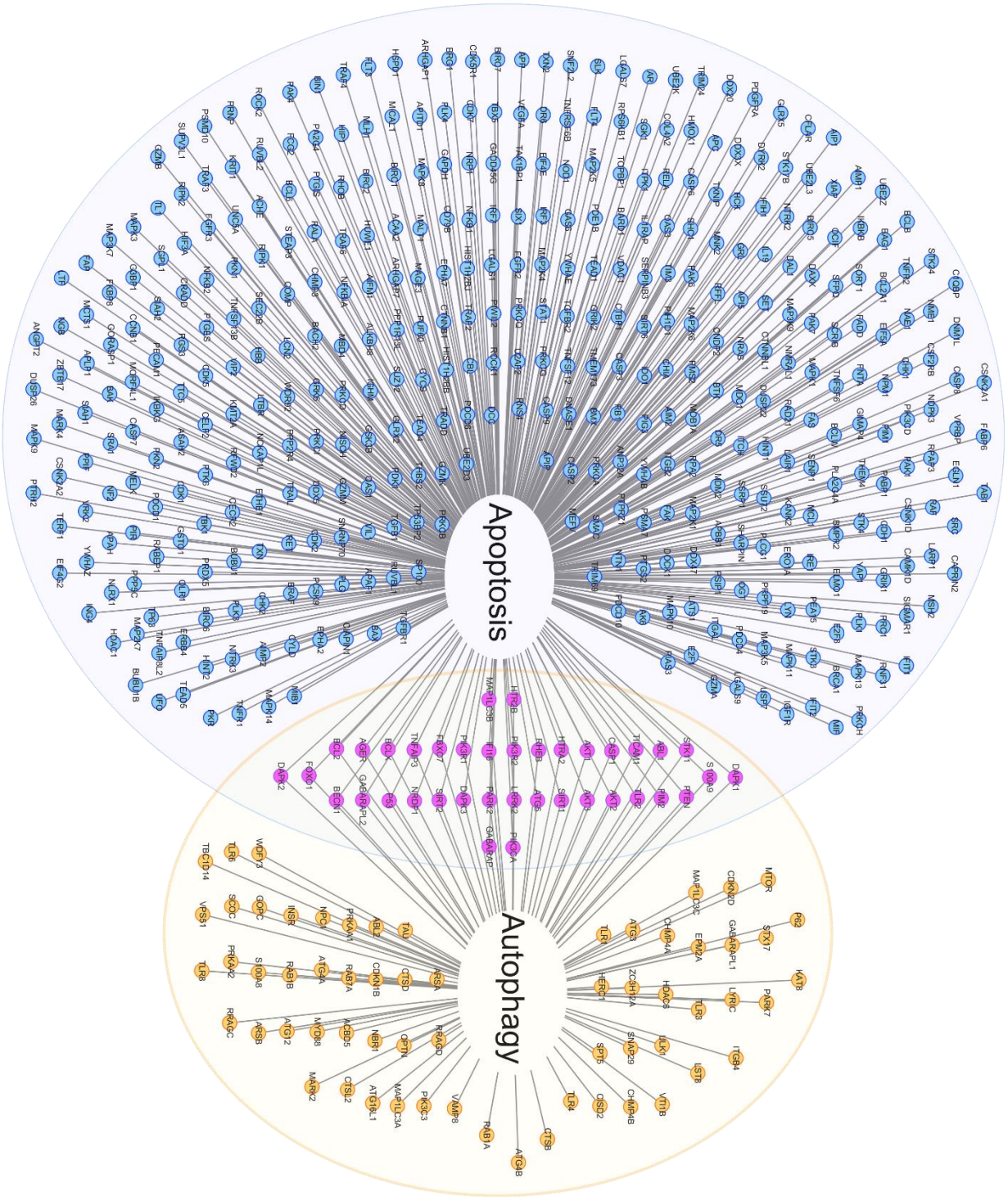

Figure 5. Targets overlap between autophagy and apoptosis.

Totally 37 targets are overlapped between autophagy and apoptosis which are ABL1, AGER, AKT1, AKT2, AKT3, ATG5, BCL2, B2CL1, BECN1, CASP1, DAPK1, DAPK2, DAPK3, FBXO7, FOXO1, GABARAP, GABARAPL2, HTR2B, HTRA2, IFI16, LRRK2, MAP1LC3B, NRDP1, P53, PARK2, PK3CA, PIK3R1, PIK3R2, PIM2, PTEN, RHEB, S100A9, SIR1, SIR2, STK11, TICAM11, TLR2 and TNFAIP3. Abbreviations: ABL1, Tyrosine-protein kinase ABL1; AGER, Advanced glycosylation end product-specific receptor; AKT1, RAC-alpha serine/threonine-protein kinase; AKT2, RAC-beta serine/threonine-protein kinase; AKT3, RAC-gamma serine/threonine-protein kinase; ATG5, Autophagy protein 5; BCL2, Apoptosis regulator Bcl-2; B2CL1, Bcl-2-like protein 1; BECN1, Beclin-1; CASP1, Caspase-1; DAPK1, Death-associated protein kinase 1; DAPK2, Death-associated protein kinase 2; DAPK3, Death-associated protein kinase 3; FBXO7, F-box only protein 7. FOXO1, Forkhead box protein O1; GABARAP, Gamma-aminobutyric acid receptor-associated protein; GABARAPL2, Gamma-aminobutyric acid receptor-associated protein-like 2; HTR2B, 5-hydroxytryptamine receptor 2B; HTRA2, Serine protease HTRA2, mitochondrial; IFI16, Gamma-interferon-inducible protein 16; LRRK2, Leucine-rich repeat serine/threonine-protein kinase 2; MAP1LC3B, Microtubule-associated proteins 1A/1B light chain 3B; NRDP1, E3 ubiquitin-protein ligase NRDP1; P53, Cellular tumor antigen p53; PARK2, E3 ubiquitin-protein ligase parkin; PK3CA, Phosphatidylinositol 4,5-bisphosphate 3-kinase catalytic subunit alpha isoform; PIK3R1, Phosphatidylinositol 3-kinase regulatory subunit alpha; PIK3R2, Phosphatidylinositol 3-kinase regulatory subunit beta; PIM2, Serine/threonine-protein kinase

pim-2; PTEN, Phosphatidylinositol 3,4,5-trisphosphate 3-phosphatase and dual-specificity protein phosphatase PTEN; RHEB, GTP-binding protein Rheb; S100A9, Protein S100-A9; SIR1, NAD-dependent protein deacetylase sirtuin-1; SIR2, NAD-dependent protein deacetylase sirtuin-2; STK11, Serine/threonine-protein kinase STK11; TICAM1, TIR domain-containing adapter molecule 1; TLR2, Toll-like receptor 2; TNFAIP3, Tumor necrosis factor alpha-induced protein 3.

3.4 Protein structure subsets and SDA calculation

3.4.1 Protein structure subsets

In order to achieve better performance of the target prediction function by HTDocking in the knowledgebases, ProSelection was used to generate the protein structure subsets. Among the targets concluded in our autophagy knowledgebases, 14 are found having enough active and inactive ligands (n≥20) in ChEMBL database (Figure 6). Related ligands are downloaded then the ProSelection was applied for these 14 targets (details were described in the method section). Eventually, 13 targets are found to have at least one PDB structure with a p value lower than 0.05. This indicates that the molecular docking process for these 13 targets is efficient enough to distinguish active ligands from inactive ones. Structures with a p value lower than 0.05 are categorized as “strong selector” structures while other structures are categorized as “weak selector” for the specific docking protocol we selected. Percentages of two categories of structures for each target in the test-set are shown in Figure 7.

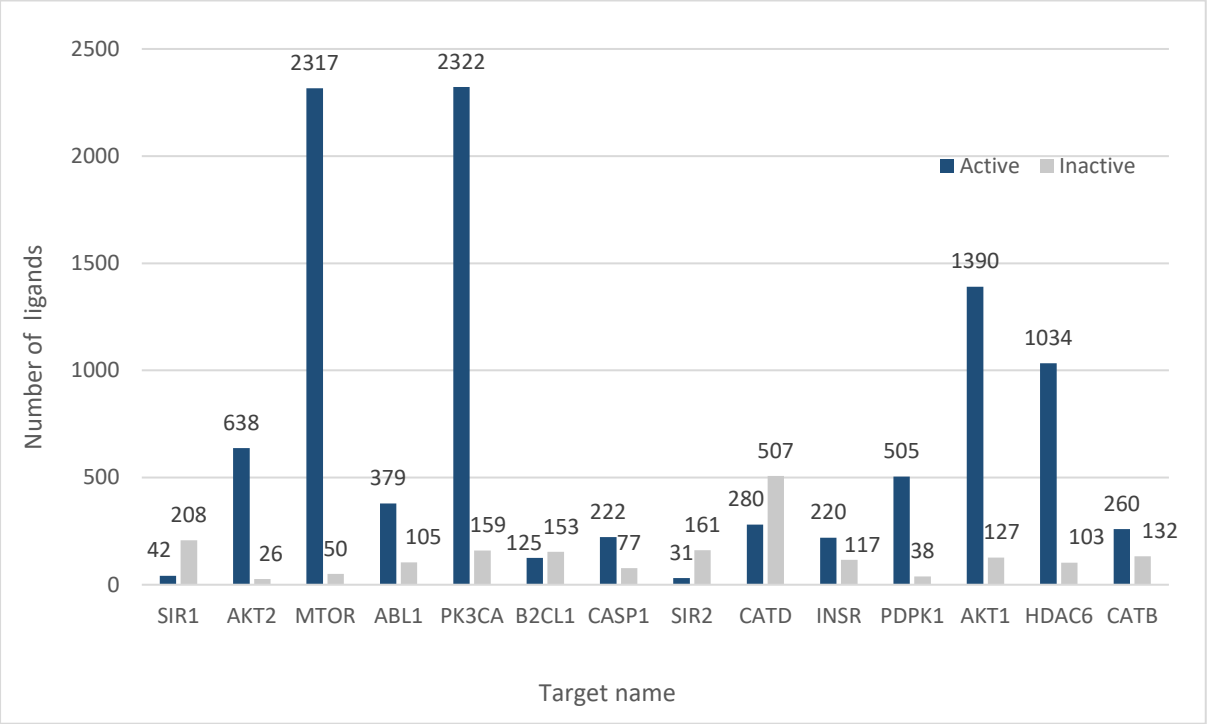

Figure 6. Ligand information for the targets in the Autophagy Knowledgebase.

Most of the targets in this protein test set have more known active ligands than inactive ligands reported in the ChEMBL database. Abbreviations: PDPK1, 3-phosphoinositide-dependent protein kinase 1; B2CL1, Bcl-2-like protein 1; CASP1, Caspase-1; CATB, Cathepsin B; CATD, Cathepsin D; HDAC6, Histone deacetylase 6; INSR, Insulin receptor; SIR1, NAD-dependent protein deacetylase sirtuin-1; SIR2, NAD-dependent protein deacetylase sirtuin-2; PK3CA, Phosphatidylinositol 4,5-bisphosphate 3-kinase catalytic subunit alpha isoform; AKT1, RAC-alpha serine/threonine-protein kinase; AKT2, RAC-beta serine/threonine-protein kinase; MTOR, Serine/threonine-protein kinase mTOR; ABL1, Tyrosine-protein kinase ABL1.

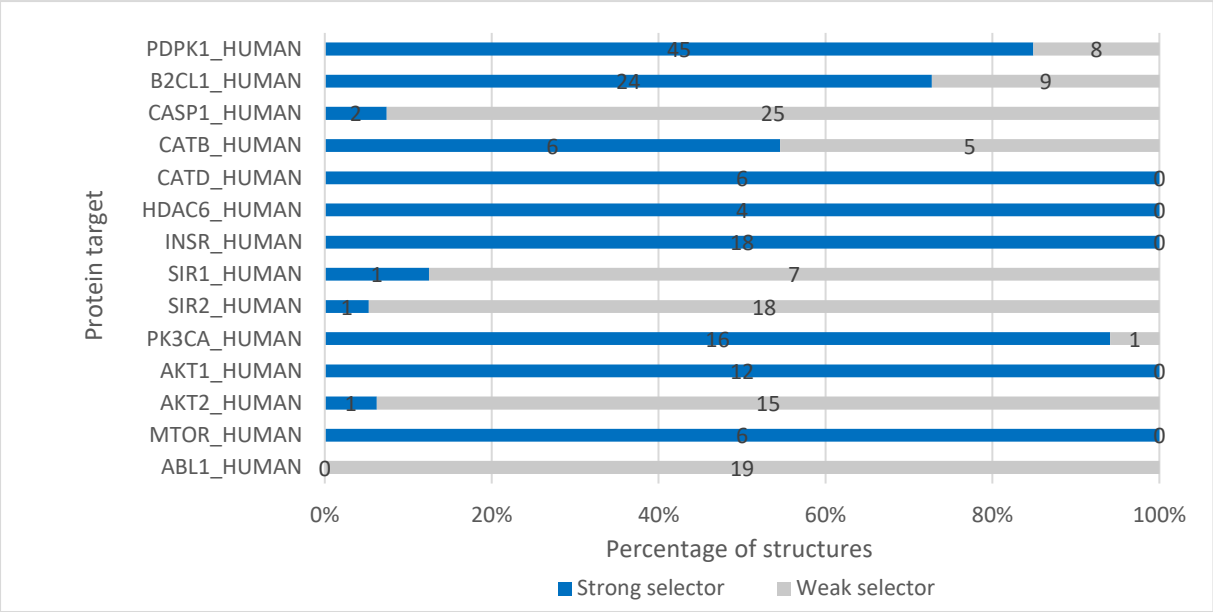

Figure 7. "Strong selector" structures in the Autophagy Knowledgebase.

Percentage of the "strong selector" structures in the Autophagy Knowledgebase. Number on the bar represents the quantity of "strong selector" or "weak selector" structures for each target.

Crystal structures which have a good performance in distinguishing active ligands from inactive ligands are labeled as "strong selector". Totally 249 PDB structures in structure test set are examined while 142 structures are "strong selector" and 107 structures are "weak selector". Among all the 14 targets in this test, thirteen targets have at least one "strong selector" structure according to ProSelection. Abbreviations: PDPK1, 3-phosphoinositide-dependent protein kinase 1; B2CL1, Bcl-2-like protein 1; CASP1, Caspase-1; CATB, Cathepsin B; CATD, Cathepsin D; HDAC6, Histone deacetylase 6; INSR, Insulin receptor; SIR1, NAD-dependent protein deacetylase sirtuin-1; SIR2, NAD-dependent protein deacetylase sirtuin-2; PK3CA, Phosphatidylinositol 4,5-bisphosphate 3-kinase

catalytic subunit alpha isoform; AKT1, RAC-alpha serine/threonine-protein kinase; AKT2, RAC-beta serine/threonine-protein kinase; MTOR, Serine/threonine-protein kinase mTOR; ABL1, Tyrosine-protein kinase ABL1.

This result suggests that for the molecular docking protocol we choose, a significant portion of PDB structures may be "weak selector" (Figure 7). These "weak selector" structures may result in unseparated docking scores against active ligands and inactive ligands during docking process. If no modifications are made either for these structures or the docking protocol, high score decoys can be expected which can be misleading for further research approaches. However, these results of the statistical selection, specifically which structure is a "strong selector" and which is a "weak selector", are docking protocol sensitive. Both the docking parameters setting and pockets definition can contribute to the selection results independently besides the protein structure itself. If other binding pockets, such as allosteric binding pockets, are used, different results of selection can be expected. For a closer look into the "weak selector" structures, several examples are used below to show why these structures are "weak selector".

Structure 3NAY and 3NAX. PDB records 3NAY and 3NAX are X-ray structures of protein PDPK1 binding to compound 2 and compound 7, which are PDPK1 inhibitors used by Jannik's group[118], respectively. In our structure selection, most of the known active ligands for this target are ATP competitive inhibitors and the typical active ATP binding site is used as the docking pocket. As a result, 3NAY is a "strong selector" structure ($p = 3.9\times$

10^{-3}) while 3NAX is labeled as "weak selector" (p = 0.12). Compound 2 in 3NAY binds to the active, DFG-in conformation of PDPK1 ATP binding site, like most typical ATP competitive inhibitors (type I). Compound 7 in 3NAX binds in the ATP pocket and induces substantial conformational changes, causing the DFG loop to exist in an "out" conformation (DFG-out) that typifies inactive form kinase inhibitors (type II)[118]. Compound 7 also disrupts the αC helix which is a unique feature to this compound among inactive form kinase inhibitors. The conformational change in the αC helix results in catalytic residue Glu-130 being displaced from the active site. This can be concluded that Compound 7 binds to the inactive kinase conformation of PDPK1 and induces conformational changes. Therefore, compared to the structure of active ATP binding site (Figure 8A), the PDPK1 protein structure co-crystalized with compound 7 is an inactive kinase conformation with some additional conformational changes which will unsurprisingly be a "weak selector" structure for active typical ATP competitive inhibitors (type I) binding (Figure 8B).

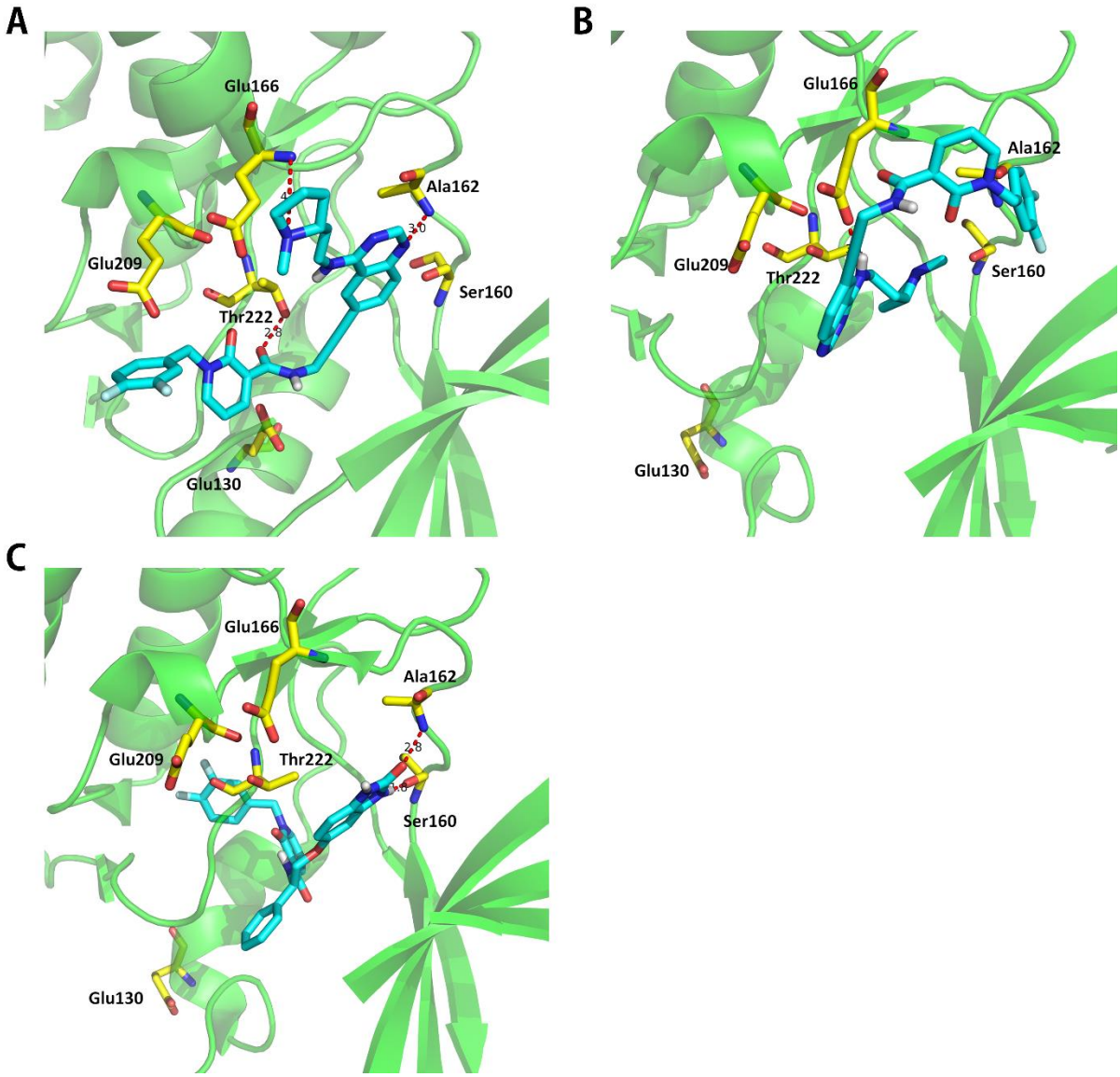

Figure 8. Compound CHEMBL3640476 binds to the PDPK1 ATP binding site

Structures of the compound CHEMBL3640476 binds to the PDPK1 ATP binding site in the kinase domain. (A) CHEMBL3640476 binds to the PDPK1 crystal structure 3NAY (Docking score 8.49). (B) CHEMBL3640476 binds to the PDPK1 crystal structure 3NAX (Docking score 5.35). (C) Original structure of 3NAX (PDPK1 co-crystalized with compound 7). Blue sticks represent the inhibitor compound CHEMBL3640476. Yellow sticks represent the important residues which are also labeled. H-bonds to the important residues are displayed as dashed red lines. In 3NAY, CHEMBL3640476 has H-bond to Ala162, Glu166, and Thr222

within the ATP-site of PDPK1. Glu130 is also in the active binding site. However, in 3NAX, only on H-bond to Glu166 is formed while Glu130 is out of the active site.

Structure 4L2Y and 4L23. PDB records 4L2Y and 4L23 are derived from the X-ray structure of PI3Kα. Structure 4L2Y is co-crystallized with compound 9d, a PI103 derivatives and known inhibitor of PI3Kα, while 4L23 is the native complex of PI103 to PI3Kα. According to the molecular modeling reported by Zhang's group[119], compound 9d would cause a decreased potency due to the electrostatic repulsion between the incoming NH2 substitute and Lys802. However, in the in vitro experiment, compound 9d was as potent as PI103 against the PI3Kα. This is because the compounds 9d can give Lys802 more flexibility which can also induce additional space at the catalytic site (Figure 9B) when compared to the original protein structure like 4L23 (Figure 9A). In our structure selection, 4L2Y is the only structure for PI3Kα which is labeled as "weak selector" ($p = 0.57$) while 4L23 is labeled as "strong selector" structure ($p = 3.6\times10^{-5}$). High p value of 4L2Y may be due to the structural change of this protein because of the co-crystallized compound 9d, particularly, a more flexible Lys802, which is one of the most important residues inside the docking pocket. Consistent with the failure of molecular docking to predict the experimental potency of 4L2Y in Zhang's group[119], the disability of our selection procedure to label this structure as "strong selector" is not surprising.

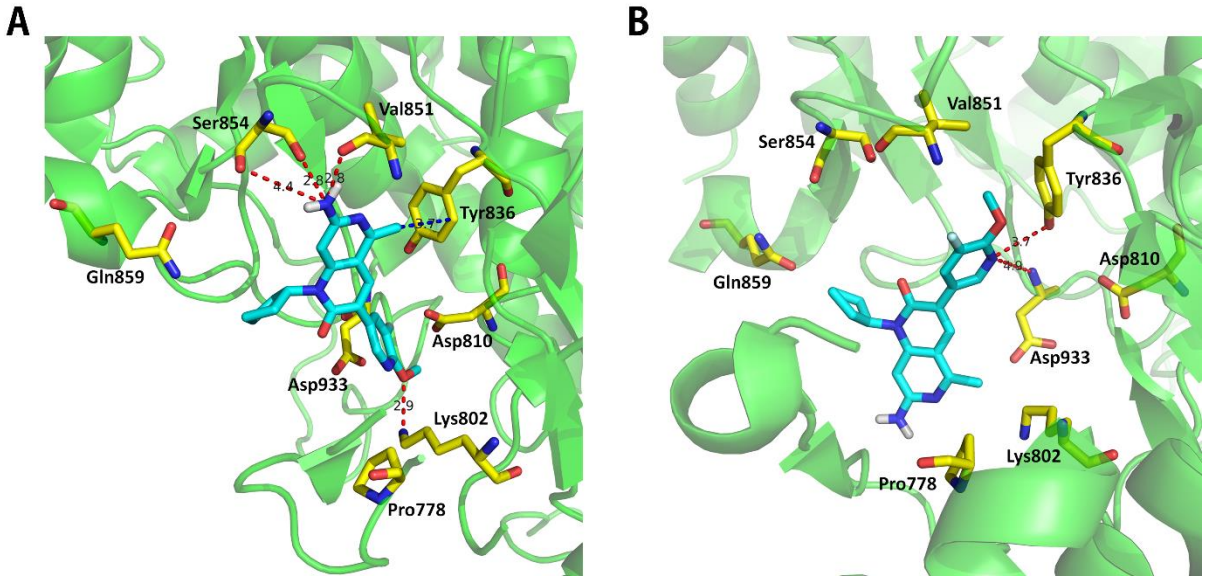

Figure 9. Compound CHEMBL3112724 binds to the kinase domain of PI3Kα.

Structures of the compound CHEMBL3112724 binds to the kinase domain in the PI3Kα. (A) CHEMBL3112724 binds to the PI3Kα crystal structure 4L23 (Docking score 9.64). (B) CHEMBL3112724 binds to the PI3Kα crystal structure 4L2Y (Docking score 5.87). Blue sticks represent the inhibitor compound CHEMBL3640476. Yellow sticks represent the important residues which are also labeled. H-bonds to the important residues are displayed as dashed red lines. In 4L23, CHEMBL3640476 has H-bond to Lys802, Val851 and Ser854 (Two H-bond). However, in 4L2Y, only two H-bond is formed between CHEMBL3112724 and PI3Kα. No H-bond for Lys802 results in the lower docking scores in molecular docking. However, this gives Lys802 more flexibility which surprisingly grants CHEMBL3112724 stronger activity.

Structure 2X39, 1MRY, and 1MRV. PDB records 2X39, 1MRY and 1MRV are structures of protein kinase B (PKB or AKT2) from X-ray. Structure 2X39 is co-crystallized

with the known inhibitor compounds 21[120], while 1MRY and 1MRV are crystal structures of an inactive Akt2 kinase domain[121]. In the structure selection, 2X39 is a "strong selector" structure (p = 0.012) compared to the 1MRY (p = 1) and 1MRV (p = 1) which are "weak selector" structures. In the docking research of 2X39, known AKT2 chemical inhibitor has H-bonds to Ala232, Glu236, Glu279 and Asp293 (Figure 10A). However, in 1MRV, only two H-bonds are formed between the inhibitor and AKT2 (Figure 10B). No H-bond is formed in 1MRY (Figure 10C). Structure 1MRV even has higher docking scores for inactive ligands when compared to active ligands. Although the reason behind this "reversed" docking score distribution still remains unknown (which may simply due to some random accidents during docking process), ProSelection has proved once again to be able to distinguish active protein conformations from inactive conformations.

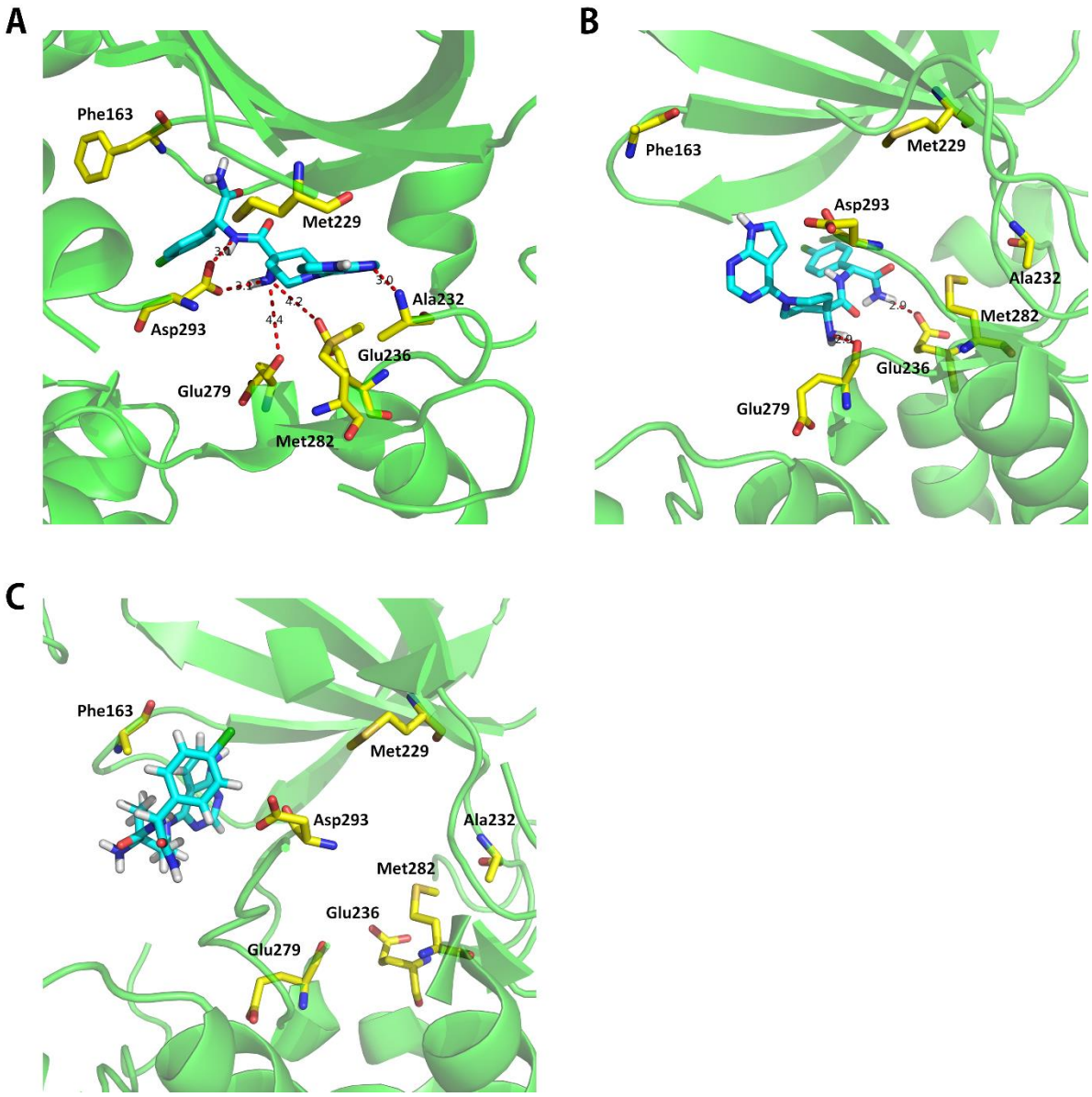

Figure 10. Compound CHEMBL2325730 binds to ATP binding site in AKT2.

Structures of the compound CHEMBL2325730 binds to the ATP binding site within the kinase domain in AKT2. (A) CHEMBL2325730 binds to the AKT2 crystal structure 2X39 (Docking score 9.11). (B) CHEMBL2325730 binds to the AKT2 crystal structure 1MRV (Docking score 3.53). (C) CHEMBL2325730 binds to the AKT2 crystal structure 1MRY (Docking score 2.66). Blue sticks represent the inhibitor compound CHEMBL2325730. Yellow sticks represent the important residues which are also labeled. H-bonds to the

important residues are displayed as dashed red lines. In 2X39, CHEMBL3640476 has H-bond to Ala232, Glu236, Glu279 and Asp293 (Two H-bond). However, in 1MRV, only two H-bond is formed between CHEMBL3112724 and AKT2. No H-bond is formed between CHEMBL3112724 and AKT2 in 1MRY.

Structure 2YXJ and 4HNJ. PDB records 2YXJ and 4HNJ are structures of the Bcl-2-like protein 1 (also named Bcl-xL) from crystallography. Bcl-xL is a potent non-kinase protein inhibitor of cell death and caspases activation. Structure 2YXJ is the crystal structure of Bcl-xL in complex with ABT-737, a known Bcl-xL inhibitor which belongs to the class of BH3 mimics. While 4HNJ is the crystallographic structure of Bcl-xL domain-swapped dimer in complex with PUMA, which induced partial unfolding of two α-helix within Bcl-xL BH3 binding pocket[122]. In our research, 2YXJ is a "strong selector" ($p = 0.029$) while 4HNJ is a "weak selector" ($p = 0.49$). This is demonstrated in the docking research where the known inhibitor of Bcl-xL forms two H-bonds to Phe150 in the BH3 binding pocket (Figure 11A). However, no H-bond is formed in the BH3 binding pocket in the 4HNJ (Figure 11B). Therefore, 4HNJ is unsurprisingly a "weak selector" for BH3 mimics because of its structural change in the BH3 binding domain induced by PUMA.

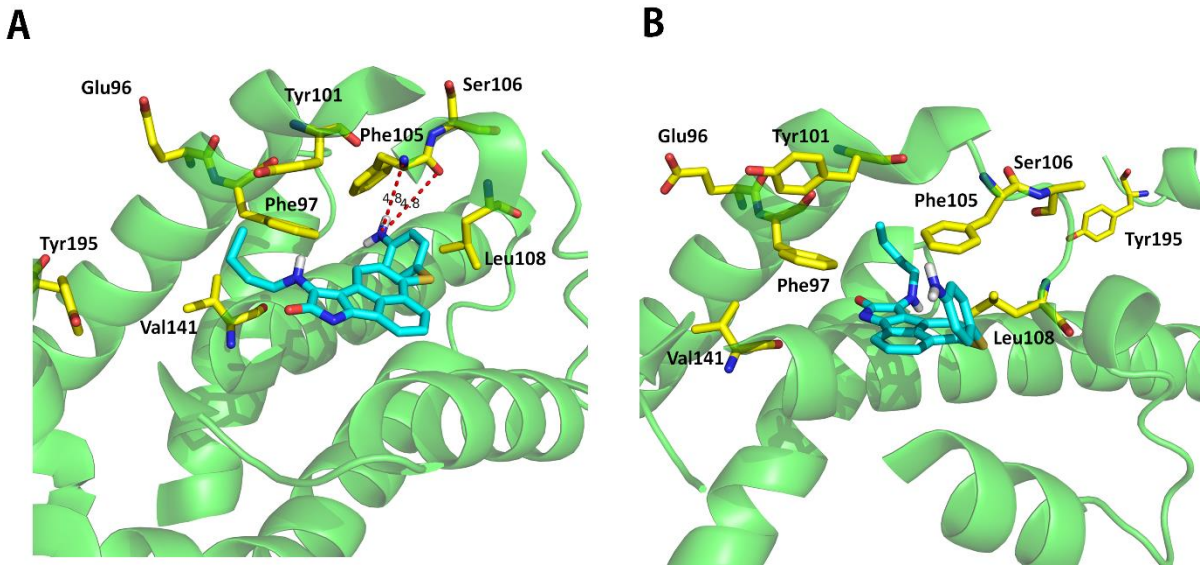

Figure 11. Compound CHEMBL2312484 binds to BH3 domain within Bcl-xL.

Structures of the compound CHEMBL2312484 binds to the BH3 binding domain within the Bcl-xL. (A) CHEMBL2312484 binds to the Bcl-xL crystal structure 2YXJ (Docking score 5.42). (B) CHEMBL2312484 binds to the Bcl-xL crystal structure 4HNJ (Docking score 2.65). Blue sticks represent the inhibitor compound CHEMBL2312484. Yellow sticks represent the important residues which are also labeled. H-bonds to the important residues are displayed as dashed red lines. In 2YXJ, CHEMBL2312484 has two H-bond to Phe105 in the BH3 binding domain. However, no H-bond is formed within the BH3 binding domain between 4HNJ and CHEMBL2312484. The residue Tyr195 in 4HNJ is even "out" of the BH3 binding domain due to the protein structural change.

Although only a small proportion of targets in our Knowledgebase have enough active and negative ligands to apply ProSelection (Figure 6), these targets, on the other hand, are commonly considered as "popular" targets. For instance, AKT, MTOR, and PK3CA (PI3K) are important targets in several pathways including the autophagy signaling (Figure 1), more

than three thousand papers are published for these targets respectively in the year of 2016. While B2CL1 (Bcl-xL), which belongs to the Bcl-2 family protein, is another important apoptosis-related target under dense research with around 600 publication in 2016 on PubMed.

3.4.2 SDA calculation

Before validating the target-predictions base on the protein structure subsets generated by ProSelection, we raise the hypothesis that each individual protein structure of a protein target may have its unique docking score distribution for even the same set of ligands. This is due to the existence of diverse protein/compound structures and docking protocols in real life. For instance, docking score of 6.0 may be high enough for those compounds against one structure to be considered as "active". However, the same score 6.0 may not be sufficient enough for another structure to determine active ligands. This further indicates that if an individual docking score criterion can be established for each structure, a better understanding of docking score in the molecular docking can be expected to distinguish active ligands from inactive ligands.

In this work, the suggested docking score threshold for active ligands (SDA) is used as score criterion for individual protein structures base on the ROC curve with both a restriction of FPR and an optimized TPR versus FPR (see more details in method section). Figure 12 presents the ROC curves for 4 of the "strong selector" structures in our structure test set. SDA is then calculated by finding the optimal cutoff points in the ROC curves for each individual crystal structure. Particularly, SDA is a new concept raised in this work which is

designed for a better understanding of the docking scores in the molecular docking research.

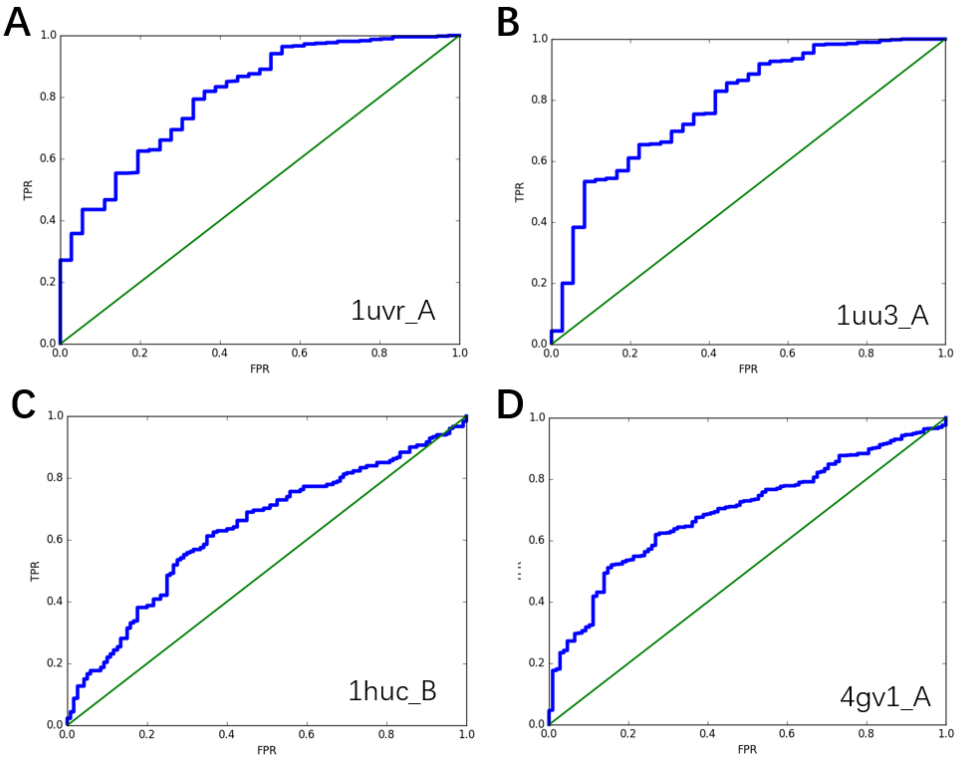

Figure 12. ROC curve of 4 "strong selector" structures.

The receiver operating characteristic (ROC) curves of one of the crystal structures of (A) 3-phosphoinositide-dependent protein kinase 1 (PDBid 1uvr, chain A, SDA = 6.27). (B) 3-phosphoinositide-dependent protein kinase 1 (PDBid 1uu3, chain A, SDA = 6.57). (C) Cathepsin B (PDBid 1huc, chain B, SDA = 5.26). (D) RAC-alpha serine/threonine-protein kinase (PDBid 4gv1, chain A, SDA = 6.14).

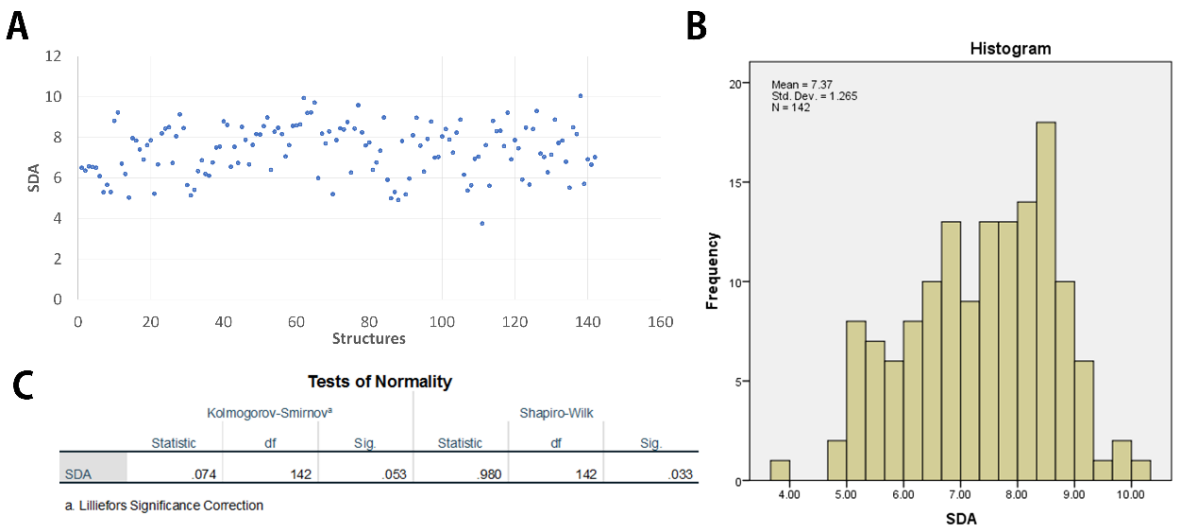

Figure 13. SDA of 142 "strong selector" structures.

(A) Suggested docking score threshold for active ligands (SDA) of 142 "strong selector" structures. (B) SDA distribution (n = 142). (C) Normality test for the SDA distribution (n = 142).

The SDAs for the 142 "strong selector" structures in the Autophagy Knowledgebase distribute from 4.0 to 10.0 (Figure 13A). It presents a non-normal distribution with a mean value of 7.37 and standard deviation of 1.265 (Figure 8B and 8C). Although most of the SDA falls in the range of 6 to 8, few reach an even higher score of 10.0 which is previously considered as "very high" in molecular docking. On the other hand, 4PPI, which belongs to the Bcl-2 family protein Bcl-xL, has a low SDA of 3.76. These results are particularly inspiring for active ligands prediction in the future. Previously, those compounds with a docking score lower than 4 will tend to be recognized as "inactive ligands" no matter which target the score is against.

3.5 Off-targets prediction using the "strong selector" structures

Target identification of small molecules is important for unraveling the underlying mechanisms of their bioactivities or side effects. Both autophagy and apoptosis are key players in the cancer therapeutics. Autophagy is considered as one of the most critical drug resistance mechanisms due to its attempt of removing damaged cellular components in the drug administered cancer cells[18]. The ability of evading apoptosis is generally recognized as one of the hallmarks of cancer [84]. As a validation procedure, we used the protein structures in the structure subsets of our Autophagy Knowledgebase to predict the potential autophagy-apoptosis related off-targets for 43 FDA-approved small molecule antineoplastic agents. Previously, 13 targets have at least one "strong selector" structure according to ProSelection. ChEMBL is then used as the source for searching the experimental IC_{50} data for the drug binding for these targets. Among these targets, insulin receptor (INSR) and histone deacetylase 6 (HDAC6), are selected for validation due to their relatively abundant data in ChEMBL database.

INSR is generally considered as a drug target for anti-hyperglycemia and the treatment of diabetes. However, it also tightly relates the phagophore formation, which is one of the early stages in the macroautophagy. Enhanced insulin signaling will inhibit the autophagy in the initiation process by inducing the downstream PI3K/AKT/mTOR pathway[123]. A molecular docking study for 43 FDA-approved antineoplastic drugs against insulin receptor was conducted (Figure 14A). In this docking process, only the 18 "strong selector" structures of insulin receptor were used. Among these 43 drugs, 6 agents have binding IC_{50} data in the ChEMBL database (Table 7) and their associated docking scores were summarized in Figure

14B.

A commonly used IC_{50} threshold for active compounds in binding assay is 10 μM[124]. Specifically, one compound can be considered as "active" once it has an IC_{50} lower than 10 μM or 10000 nM. Osimertinib is an "active" compound for INSR in the experiment (Table 7) and it shows a docking score higher than SDA for 8 of total 18 INSR structures in the molecular docking after ProSelection. Similar result was also observed for the "active" drug Crizotinib, Ceritinib and Sunitinib. However, for "inactive" compounds like Lapatinib, scores against some structures are unexpectedly higher than SDA (Figure 14B). This is acceptable due to the fact that molecular docking has some extent of "randomness"[125] and most of the inactive compounds in our test have a lower quantity of high scores ($< \frac{1}{3}$ all available structures) compared to active compounds ($\geq \frac{1}{3}$ all available structures). On the functional level, drugs inhibit the INSR will further inhibit the downstream signaling of PI3K/AKT/mTOR pathway. An enhancement of autophagy function can be observed as the final result of this signaling, which is consistent to the autophagy-related drug resistant nature of many antineoplastic agents[18].

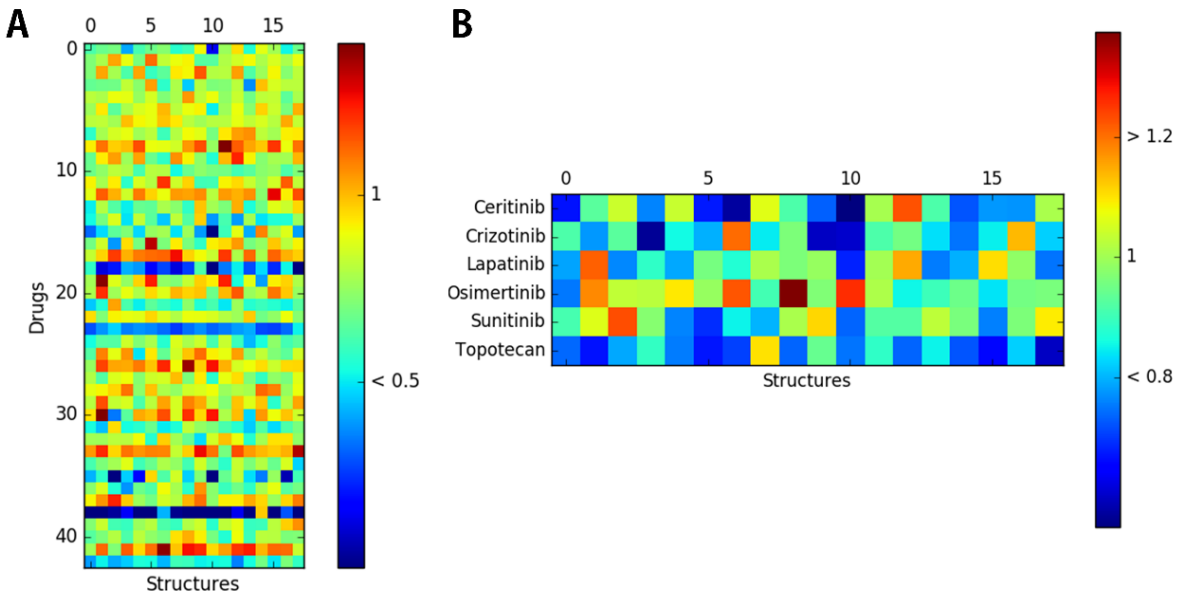

Figure 14. Docking results for FDA-approved drugs against insulin receptor.

(A) Docking scores for 43 FDA-approved antineoplastic drugs. (B) Docking scores for 6 FDA-approved drugs with experimental binding data in ChEMBL. All docking scores are shown in folds compared to the corresponding suggested docking score threshold for active ligands (SDA) for each structure.

Table 7. Experimental binding IC_{50} for 6 drugs against insulin receptor

Drug	**Ceritinib**	**Crizotinib**	**Lapatinib**	**Osimertinib**	**Sunitinib**	**Topotecan**
IC_{50} (nM)	7	102	17000	912	3200	Not Active
Description	Inhibition	Inhibition	Inhibition	Inhibition	Inhibition	-
Organism	Home sapiens	Home sapiens	Home sapiens	Home sapiens	Home sapiens	Home sapiens
Ref	126	127	128	129	130	-

HDAC6 is another target which closely related to autophagy. Autophagy acts as a compensatory degradation system when the ubiquitin-proteasome system (UPS) is impaired.

Histone deacetylase 6 (HDAC6), a microtubule-associated deacetylase that interacts with polyubiquitinated proteins, is an essential mechanistic link in this compensatory interaction[131]. Although HDAC6 is not required for autophagy activation, it rather controls the fusion of autophagosomes to lysosomes[132]. Molecular docking results of 43 FDA-approved antineoplastic drugs against HDAC6 was presented in Figure 15A. Again, only the "strong selector" structures are used. Belinostat, Panobinostat, and Bendamustine are known to bind HDAC6 with IC_{50} of 15, 11 and 6 nM respectively (Table 8). Belinostat and Panobinostat are successfully predicted by "strong selector" structures while Bendamustine is accidentally predicted as "inactive" (Figure 15B). For known HDAC6 "inactive" drugs Lapatinib and Romidepsin, none of the "strong selector" structures show a docking score higher than SDA (Figure 15B). These results indicate that the protein structures selected by ProSelection work accurately during active ligands prediction.

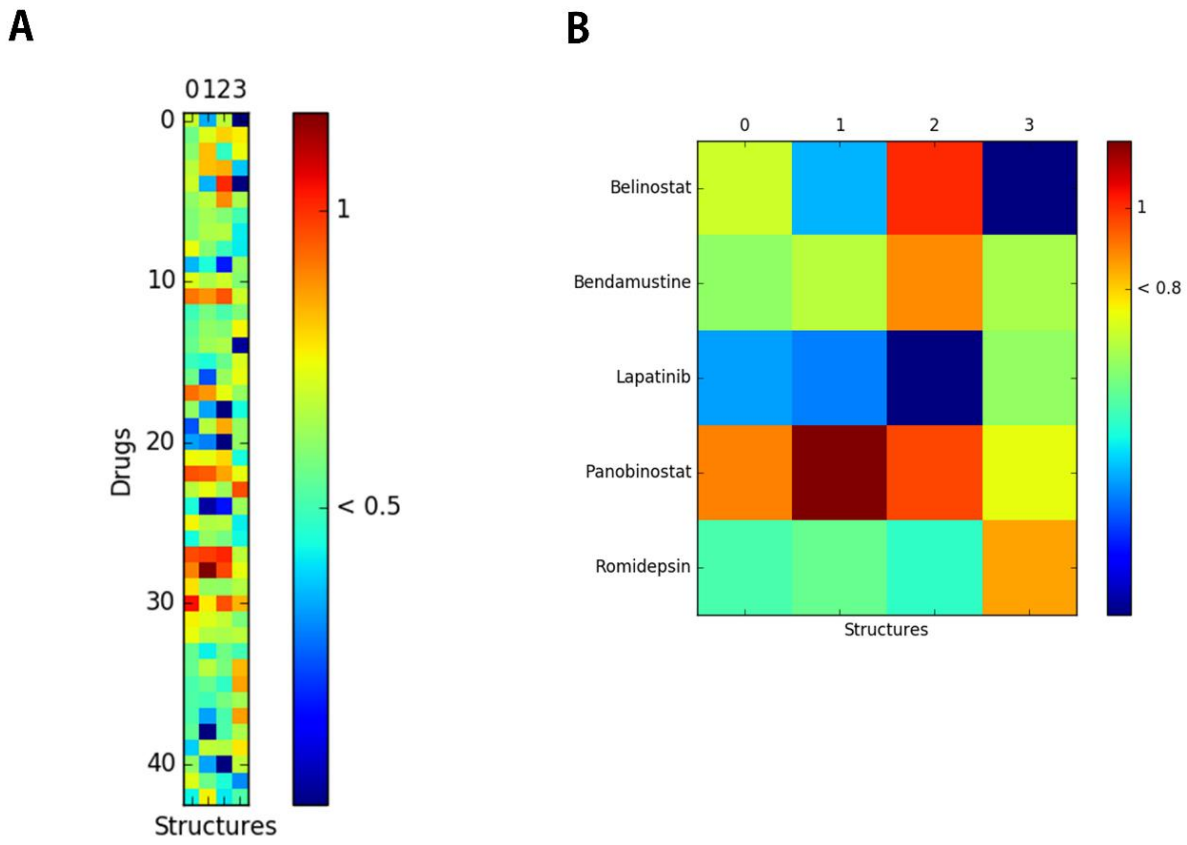

Figure 15. Docking results for FDA-approved drugs against histone deacetylase 6

(A) Docking scores for 43 FDA-approved antineoplastic drugs. (B) Docking scores for 5 FDA-approved drugs with experimental binding data in ChEMBL. All docking scores are shown in folds compared to the corresponding SDA for each structure. Scores lower than 0 are manipulated to 0 for figure generating.

Table 8. Experimental binding IC_{50} for 5 drugs against Histone deacetylase 6

Drug	Belinostat	Bendamustine	Lapatinib	Panobinostat	Romidepsin
IC_{50} (nM)	15	6	>10000	11	14000
Description	Inhibition	-	Inhibition	Inhibition	Inhibition
Organism	Homo sapiens	Homo sapiens	Homo sapiens	Homo sapiens	Homo sapiens
Ref	133	BindingDB: 7095	128	134	135

4. DISCUSSION

As is discussed in the introduction section, both autophagy and apoptosis are basic but critical in the maintenance of cellular homeostasis. The disruption of either the autophagy or the apoptosis is considered as one of the major contributors to cancer and neurological disorder. Most of the drugs now in the market are thought to interact with both autophagy and apoptosis either by a direct signaling cascade or an indirect functional regulation. However, this can be particularly challenging when the regulations of autophagy and apoptosis by a medication are in the opposite directions. Specifically, one drug may inhibit the growth of cancer in the aspect of apoptosis but facilitate the cancer survival at the same time in the aspect of autophagy. Therefore, specific knowledgebases for autophagy and apoptosis are expected to be beneficial for the research which are related to cancer and neurological disease.

With the construction of the Autophagy-apoptosis specific knowledgebases in this work, one can have a specific overview of autophagy and apoptosis from molecular signaling level to the chemical level. These knowledgebases integrate several system pharmacological analysis tools including but not limit to HTDocking, BBB predictor, PAIN remover, and Toxicity predictor, which will further accelerate the autophagy-apoptosis related research by using the information collected in the knowledgebase. Several shared protein targets between autophagy and apoptosis are also revealed by the overlapping study between these two knowledgebases. These targets are significantly important due to their potential dual functions in the diseases and disease-related treatment. Researchers who plan to treat the

diseases by manipulating the autophagy or apoptosis function can take great benefits from these knowledgebases, either by the information searching or the target prediction.

When combined with the ProSelection, a computational statistical selection for generating the proper protein structure subset based on the research purpose, the performance of target prediction of the Autophagy Knowledgebase and Apoptosis Knowledgebase has been measured by using targets associated active and inactive ligands. In this study 249 crystal protein structures from 14 autophagy or apoptosis related targets were examined. Either two independent t-test or Mann-Whitney U test was used to distinguish "strong selector" structures from "weak selector" structures base on the normality of the docking score distribution for each individual protein structure. The receiver operating characteristic (ROC) curve has been made and suggested docking scores threshold for active ligands (SDA) were generated for each "strong selector" structure according to the ROC curve. The performance of target prediction base on the "strong selector" structures was validated by FDA recently approved small molecule antineoplastic drugs for predicting their off-targets among autophagy or apoptosis related proteins.

Several autophagy or apoptosis related databases are now available online, popular ones including but not limited to the iLIR Autophagy Database (http://ilir.warwick.ac.uk/), the Autophagy DB, HADb (http://www.autophagy.lu/), Deathbase (http://www.deathbase.org/), and The Apoptosis Database[136]. All of these public databases serve as good information portals for searching autophagy-apoptosis related protein, pathway, and gene information. Compared to these databases, the knowledgebases reported in this thesis contain not only the autophagy-apoptosis related information but also some practical tools for chemoinformatics

research. This will grant the researchers a better convenience when conducting the autophagy-apoptosis related drug development.

5. CONCLUSION AND FUTURE SPECULATION

In this study, we established two knowledgebases which are specifically designed for autophagy or apoptosis by collecting the related gene, protein, and chemical data with several chemoinformatics tools integrated. We used our knowledgebase to review the important drug targets in autophagy and apoptosis research paired with their known chemical modulators in the clinical studies. Target overlap study was also conducted based on these knowledgebases to investigate the potential interaction between autophagy and apoptosis. Target prediction function was also implemented into these knowledgebases by using the open-source algorithm and the proper protein structure subsets. Overall, the Autophagy Knowledgebase and the Apoptosis Knowledgebase will accelerate our work in disease-specific information acquiring and could be a useful tool for predicting the potential targets for future medications.

It is worth considering the weaknesses of this current study to explore the directions for further research. The generation of the proper protein structure subsets in these knowledgebases is highly dependent on the abundance of known active and inactive ligands. As shown in Figure 6, number of active ligands is usually much larger than inactive ligands in the public databases. This ratio can even approach 50 for some targets. One solution is to replace the inactive ligands with random ligands. This is expected to lower the performance of the structure selection because of the existence of active ligands in a random compound-set. However, this is still acceptable because a “strong selector” structure is also expected to

distinguish active ligands from random ligands. More importantly, the number of random compounds is not limited. More protein targets will be available for predicting if only active and random compound-set are used. Specifically, every target with the size of active ligand test-set larger than 20 is sufficient for ProSelection if random ligands set is used. However, for targets which do not have enough active ligands, statistical approaches like ProSelection will no longer be able to use. Therefore, machine learning algorithms can be an alternative solution to predict the proper protein structure subset base on the similar logic of designing ProSelection. This potential upgrade of ProSelection will bring the Autophagy Knowledgebase and Apoptosis Knowledgebase more accuracy when predicting the targets.

A further consideration in these knowledgebases is the collaboration of ProSelection with ensemble docking. Because of the backstage usage of popular docking tools like Sybyl-x and Autodock Vina, statistical methods like ProSelection are still categorized as “rigid” docking but with flexible ligands. If ensemble docking (which has taken receptor flexibility into consideration) can be integrated into ProSelection, a much better performance is expected because of the consideration of the flexibility in both the protein target and the ligand.

APPENDIX. CORE CODES

Following codes are principle codes for the ProSelection in the Linux system.

The code for this section was written in extract_name_1.py using Python language:

```
# this file will extract pdbIDs from original file from Autophagy Knowledgebase then create 4 new summary files: ids_names.csv, names_ids.csv, name_summary.csv, idsWITHchain.csv.


#!/usr/bin/python
from os import walk
import sys, os, re, operator, requests


# create list of file names in the input dictionary
filenamelist = []
for (dirpath, dirnames, filenames) in walk('./ligands/'):
        filenamelist.extend(filenames)
        break


# read files in the input dictionary
pdbidlist= []
pdbid_chain = []
for filename in filenamelist:
        regex1 = re.compile(r'(\S+?)_[A-Z]+?_')
        result1 = regex1.findall(filename)
        pdbidlist.append(result1)
      regex2 = re.compile(r'(\S+)_[AN]+?-results')
        result2 = regex2.findall(filename)
```

```
        pdbid_chain.append(result2)
pdbid_chain=sorted(pdbid_chain)


# delete duplicates in pdbids
def uniq(lst):
        last = object()
        for item in lst:
                if item == last:
                        continue
                yield item
                last = item
def sort_and_deduplicate(l):
        return list(uniq(sorted(l, reverse=True)))
pdbidlist1 = sort_and_deduplicate(pdbidlist)


f = open('./reports/idsWITHchain.txt', 'w')
for line in pdbid_chain:
        f.write(line[0]+'\n')
f.close()


# print out the id with associated protein name
comlist= []
i=1
for id in pdbidlist1:
        url=id[0]
        contents = requests.get('http://www.rcsb.org/pdb/rest/describeMol?structureId='+url).text
        regex1 = re.compile(r'<macroMolecule name=\"([\S\s]+?)\">')
        result1 = regex1.findall(contents)
```

```
    try:
            tup = (url,result1[0])
     except:
        tup = (url,'0')
     comlist.append(tup)
     print str(i)+' pdbID finished! '
     i=i+1

# sort results
done=sorted(comlist, key=operator.itemgetter(0))
done1=sorted(comlist, key=operator.itemgetter(1))
print 'ids_names.csv length: '+str(len(done))+'\n','names_ids.csv length: '+str(len(done1))

# write to file
f = open('./reports/ids_names.txt', 'w')
for line in done:
     f.write(line[0]+'       '+line[1]+'\n')
f.close()

proteinlist = []
f = open('./reports/names_ids.txt', 'w')
for line in done1:
     proteinlist.append(line[1])
     f.write(line[1]+'       '+line[0]+'\n')
f.close()
prolist_ndup = sort_and_deduplicate(proteinlist)
```

```
f = open('./reports/name_summary.txt', 'w')
for target in prolist_ndup:
    f.write(target)
    for duptarget in comlist:
        if duptarget[1]==target:
            f.write('    '+duptarget[0])
    f.write('\n')
f.close()
print ' extract_name_1.py Done! '
```

The code for this section was written in mod_scores_2.py using Python language:

```
# this file will modify raw docking score files in 'ligands' and save them to new files in 'ligands_mod'
with a simpler name

#!/usr/bin/python
from os import walk
import sys, urllib2, os, re, operator

# create file name list
filenamelist = []
for (dirpath, dirnames, filenames) in walk('./ligands/'):
    filenamelist.extend(filenames)
    break
```

```
# processing raw docking score files
for name in filenamelist:
    f = open('./ligands/'+name, 'r')
    regex1 = re.compile(r'(\S+?)-results')
    result1 = regex1.findall(name)
    f1 = open('./ligands_mod/'+result1[0]+'.csv', 'w')
    f1.write('compounds,score,activity\n')
    for line in f:
      if line.find('_000') != -1:
          regex2 = re.compile(r'([\S\s]+?)_000')
          result2 = regex2.findall(line)
          regex3 = re.compile(r'_000 (\S+?) ')
          result3 = regex3.findall(line)
          regex4 = re.compile(r'_([A-Z]+?)-results')
          result4 = regex4.findall(name)
          if result4[0]=='A':
              f1.write(result2[0]+','+result3[0]+','+'1'+'\n')
          else:
              f1.write(result2[0]+','+result3[0]+','+'0'+'\n')
    f.close()
    f1.close()
print ' mod_scores_2.py Done! '
```

The code for this section was written in spss_scores_3.py using Python language:

```
# this file will further process dockingscore data in 'ligands_mod' and only extract the scores then save
under 'spss_score' with simplist name


#!/usr/bin/python
from os import walk
import re


# create file name list
filenamelist = []
for (dirpath, dirnames, filenames) in walk('./ligands_mod/'):
    filenamelist.extend(filenames)
    break


for name in filenamelist:
    f0 = open('./ligands_mod/'+name,'r')
    header=f0.readline()
    regex1 = re.compile(r'(\S+?).csv')
    result1 = regex1.findall(name)
    f1 = open('./spss_scores/'+result1[0],'w')
    for line in f0:
        sline=line.split(',')
        f1.write(sline[1]+'\n')
    f0.close()
    f1.close()


print ' spss_scores_3.py Done! '
```

The code for this section was written in mann_whitney_4.py using Python language:

```
# this file use the numeric data in 'spss_scores' to run Mann-Whitney test or t-test to see wether the mean of scores for active and inactive ligands are significantly different with each other.


#!/usr/bin/python
from os import walk
import scipy
from scipy.stats import *
import re


# create file name list
filenamelist = []
for (dirpath, dirnames, filenames) in walk('./spss_scores/'):
    filenamelist.extend(filenames)
    break


pdbidlist= []
for filename in filenamelist:
    regex1 = re.compile(r'(\S+?_[A-Z]+?)_[AN]+?')
    result1 = regex1.findall(filename)
    pdbidlist.append(result1[0])


# create list of uniq pdbid with chains
def uniq(lst):
    last = object()
    for item in lst:
        if item == last:
            continue
```

```
            yield item
            last = item
def sort_and_deduplicate(l):
    return list(uniq(sorted(l)))
pdbidlist1 = sort_and_deduplicate(pdbidlist)


# mann-whitney test and t-test. need sample size for each sample is larger than 20
f2 = open('./reports/mann-whitney_result.csv','w')
f2.write('pdbID,normtest_A,normtest_N,p-value,test\n')
for item in pdbidlist1:
    f0 = open('./spss_scores/'+item+'_A','r')
    f1 = open('./spss_scores/'+item+'_N','r')
    actives=[]
    negtives=[]
    for score1 in f0:
        score1=score1.split('\n')
        actives.append(float(score1[0]))
    for score2 in f1:
        score2=score2.split('\n')
        negtives.append(float(score2[0]))
    if len(actives)>=20 and len(negtives)>=20:
        k2a,pa =scipy.stats.normaltest(actives,axis=0)
        k2n,pn =scipy.stats.normaltest(negtives,axis=0)
        if pa >= 0.05 and pn >= 0.05:
            mw_result=scipy.stats.ttest_ind(actives, negtives, equal_var=False)
            p_value=(mw_result[1])/2
            test='t'
        else:
            mw_result=scipy.stats.mannwhitneyu(actives, negtives, use_continuity=True,
alternative='greater')
```

```
            p_value=mw_result[1]
            test='m'
        f2.write(str(item)+','+str(pa)+','+str(pn)+','+str(p_value)+','+test+'\n')
    else:
        f2.write(str(item)+','+'Ligands not enough,Ligands not enough,Ligands not enough'+'\n')
    f0.close()
    f1.close()
f2.close()
print ' mann_whitney_4.py compeleted! '
```

The code for this section was written in bonferroni_5.py using Python language:

```
# this file will apply Bonferroni correction on the original p value from statistical test


#!/usr/bin/python
from os import walk
import sys, urllib2, os, re, operator


f0 = open('reports/mann-whitney_result.csv','r')
f0.readline()
f1 = open('reports/name_summary.txt','r')
f2 = open('reports/bonferroni.txt','w')
f2.write('pdbID       p_value    bonferroni       pOK structures\n')


# Create guide for bonferroni divide
guide={}
```

```
for line in f1:
    line=line.rstrip('\n').split('   ')
    i=1
    while i<len(line):
        guide[line[i]]=len(line)-1
        i=i+1


# cal
for line in f0:
    line=line.rstrip('\n').split(',')
    regex0 = re.compile(r'(\S+?)_')
    result0 = regex0.findall(line[0])
    if line[1]=='Ligands not enough':
        f2.write(line[0]+'     '+line[3]+'       NA   0\n')


    else:
        p = float(line[3])
        k = float(guide[result0[0]])
        bon = 1-((1-p)**k)
        if bon <= 0.05:
            f2.write(line[0]+' '+line[3]+'       '+str(bon)+'     1      '+str(k)+'\n')
        else:
            f2.write(line[0]+' '+line[3]+'       '+str(bon)+'     0      '+str(k)+'\n')
f0.close()
f1.close()
f2.close()
print ' bonferroni_5.py Done! '
```

The code for this section was written in roc_6.py using Python language:

```
# this file will generate roc curve for the protein structures in the test


#!/usr/bin/python
from os import walk
from sklearn.metrics import *
from shutil import copyfile
import matplotlib.pyplot as plt
import sys, urllib2, os, re, operator
import numpy as np


# create list of idwithchain
f0=open('./reports/idsWITHchain.txt','r')
idchain0=[]
for line in f0:
    line=line.rstrip('\n')
    idchain0.append(line)
def uniq(lst):
    last = object()
    for item in lst:
        if item == last:
            continue
        yield item
        last = item
```

```
def sort_and_deduplicate(l):
    return list(uniq(sorted(l)))
idchain = sort_and_deduplicate(idchain0)
f0.close()


# create rawfile in roc folder
for line in idchain:
    f3=open('./roc/'+line+'.csv','w')
    f1=open('./spss_scores/'+line+'_A','r')
    f2=open('./spss_scores/'+line+'_N','r')
    for line1 in f1:
        line1=line1.rstrip('\n')
        f3.write(line+','+line1+','+'1\n')
    for line2 in f2:
        line2=line2.rstrip('\n')
        f3.write(line+','+line2+','+'0\n')
    f1.close()
    f2.close()
    f3.close()


filenamelist = []
for (dirpath, dirnames, filenames) in walk('./roc/'):
    filenamelist.extend(filenames)
    break
```

```
# create roc for all pdbIDs
c=0
for filename in filenamelist:
    true=[]
    score=[]
    f4=open('./roc/'+filename,'r')
    for line3 in f4:
        line3=line3.rstrip('\n').split(',')
        true.append(float(line3[2]))
        score.append(float(line3[1]))
        name=line3[0]
    true=np.array(true)
    score=np.array(score)
    fpr, tpr, thresholds=roc_curve(true,score,pos_label=1)
    plt.plot(fpr,tpr,linewidth=4,clip_on=False)
    plt.plot([0,1],[0,1],linewidth=2,clip_on=False)
    plt.xlabel("FPR"); plt.ylabel("TPR")
    plt.ylim(0,1); plt.xlim(0,1)
    plt.savefig('./reports/roc_fig/'+name+'.png')
    plt.close()
    c=c+1
    f4.close()
    print str(c)+' pdbID finished!'
```

```
#extract figure p<0.05
f5=open('./reports/bonferroni.txt','r')
f5.readline()
for line4 in f5:
    line4=line4.rstrip('\n').split('       ')
    if float(line4[3])==1:
        copyfile('./reports/roc_fig/'+line4[0]+'.png', './reports/roc_fig/rocp/'+line4[0]+'.png')
f5.close
print ' file copied!'
```

The code for this section was written in check_mean_7.py using Python language:

```
# this file will check the mean of the docking scores to make sure the scores for active ligands are higher

#!/usr/bin/python
from os import walk
from sklearn.metrics import *
from shutil import copyfile
import matplotlib.pyplot as plt
import sys, urllib2, os, re, operator
import numpy as np
```

```
f0=open('./reports/bonferroni.txt','r')
f0.readline()
f3=open('./reports/bonferroni_P.txt','w')
f3.write('pdbID       mann-whitney bonferroni       mean_A   mean_N  p_mean\n')
for line in f0:
    line=line.rstrip('\n').split('   ')
    if float(line[3])==1:
        f1=open('./spss_scores/'+line[0]+'_A','r')
        f2=open('./spss_scores/'+line[0]+'_N','r')
        score_A=[]
        score_N=[]
        for line1 in f1:
            line1=line1.rstrip('\n')
            score_A.append(float(line1))
        for line2 in f2:
            line2=line2.rstrip('\n')
            score_N.append(float(line2))
        mean_A=np.mean(score_A)
        mean_N=np.mean(score_N)
        f1.close()
        f2.close()
        if mean_A>mean_N:
            f3.write(line[0]+' '+line[1]+'       '+line[2]+'       '+str(mean_A)+'      '+str(mean_N)+'
        1\n')
f0.close()
f3.close()
print ' check_mean_7 done!'
```

The code for this section was written in oc_cutoff_8.py using Python language:

```
# this file will generate the SDA for every strong selector


#!/usr/bin/python
from sklearn.metrics import *
import sys, urllib2, os, re, operator, math
import numpy as np


# create list of pdb for cut off making
f0=open('./reports/bonferroni_P.txt')
f0.readline()
filenamelist=[]
for line in f0:
    line=line.rstrip('\n').split('   ')
    filenamelist.append(line[0])
f0.close()


# calculate cut off based on the top-left point
f2=open('./reports/roc_cutoff.csv','w')
f2.write('pdbID,thresholds,tpr,fpr\n')
for filename in filenamelist:
    dislist=[]
    compare=[]
    true=[]
    score=[]
    f1=open('./roc/'+filename+'.csv','r')
```

```
    for line1 in f1:
        line1=line1.rstrip('\n').split(',')
        true.append(float(line1[2]))
        score.append(float(line1[1]))
        name=line1[0]
    true=np.array(true)
    score=np.array(score)
    fpr, tpr, thresholds=roc_curve(true,score,pos_label=1)
    i=0
    while i<len(tpr):
        if fpr[i]**3<=0.0001:
            distance=math.sqrt((1-tpr[i])**2+(fpr[i])**2)
            tup=(thresholds[i],distance,tpr[i],fpr[i])
            dislist.append(tup)
            compare.append(distance)
        i=i+1
    f1.close()
    mindis=min(compare)
    for tup in dislist:
        if tup[1]==mindis:
            f2.write(filename+','+str(tup[0])+','+str(tup[2])+','+str(tup[3])+'\n')
f2.close()
print ' roc_cutoff_8 done!'
```

The code for this section was written in main.py using Python language:

```
# this is an ensembled file to run all the previous code in one-step.


#!/usr/bin/python
import extract_name_1
import mod_scores_2
import spss_scores_3
import mann_whitney_4
import bonferroni_5
import roc_6
import check_mean_7
import roc_cutoff_8
import os
os.system("find . -name '*.pyc' -delete"); print ' .pyc files deleted! '
```

BIBLIOGRAPHY

1. Levine, B.; Kroemer, G., Autophagy in the pathogenesis of disease. *Cell* **2008**, 132, 27-42.

2. Mizushima, N.; Levine, B., Autophagy in mammalian development and differentiation. *Nature cell biology* **2010**, 12, 823-830.

3. Kuma, A.; Mizushima, N. Physiological role of autophagy as an intracellular recycling system: with an emphasis on nutrient metabolism. In Seminars in cell & developmental biology, 2010; Elsevier: 2010; Vol. 21; pp 683-690.

4. García-Arencibia, M.; Hochfeld, W. E.; Toh, P. P.; Rubinsztein, D. C. Autophagy, a guardian against neurodegeneration. In Seminars in cell & developmental biology, 2010; Elsevier: 2010; Vol. 21; pp 691-698.

5. White, E., Deconvoluting the context-dependent role for autophagy in cancer. *Nature Reviews Cancer* **2012**, 12, 401-410.

6. Schwarze, P. E.; Seglen, P. O., Reduced autophagic activity, improved protein balance and enhanced in vitro survival of hepatocytes isolated from carcinogen-treated rats. *Experimental cell research* **1985**, 157, 15-28.

7. Komatsu, M.; Waguri, S.; Koike, M.; Sou, Y.-s.; Ueno, T.; Hara, T.; Mizushima, N.; Iwata, J.-i.; Ezaki, J.; Murata, S., Homeostatic levels of p62 control cytoplasmic inclusion body formation in autophagy-deficient mice. *Cell* **2007**, 131, 1149-1163.

8. Komatsu, M.; Waguri, S.; Ueno, T.; Iwata, J.; Murata, S.; Tanida, I.; Ezaki, J.; Mizushima, N.; Ohsumi, Y.;

Uchiyama, Y., Impairment of starvation-induced and constitutive autophagy in Atg7-deficient mice. *J Cell Biol* **2005**, 169, 425-434.

9. Mathew, R.; Karp, C. M.; Beaudoin, B.; Vuong, N.; Chen, G.; Chen, H.-Y.; Bray, K.; Reddy, A.; Bhanot, G.; Gelinas, C., Autophagy suppresses tumorigenesis through elimination of p62. *Cell* **2009**, 137, 1062-1075.

10. Degenhardt, K.; Mathew, R.; Beaudoin, B.; Bray, K.; Anderson, D.; Chen, G.; Mukherjee, C.; Shi, Y.; Gélinas, C.; Fan, Y., Autophagy promotes tumor cell survival and restricts necrosis, inflammation, and tumorigenesis. *Cancer cell* **2006**, 10, 51-64.

11. Hara, T.; Nakamura, K.; Matsui, M.; Yamamoto, A.; Nakahara, Y.; Suzuki-Migishima, R.; Yokoyama, M.; Mishima, K.; Saito, I.; Okano, H., Suppression of basal autophagy in neural cells causes neurodegenerative disease in mice. *Nature* **2006**, 441, 885-889.

12. Mathew, R.; Kongara, S.; Beaudoin, B.; Karp, C. M.; Bray, K.; Degenhardt, K.; Chen, G.; Jin, S.; White, E., Autophagy suppresses tumor progression by limiting chromosomal instability. *Genes & development* **2007**, 21, 1367-1381.

13. Lum, J. J.; Bauer, D. E.; Kong, M.; Harris, M. H.; Li, C.; Lindsten, T.; Thompson, C. B., Growth factor regulation of autophagy and cell survival in the absence of apoptosis. *Cell* **2005**, 120, 237-248.

14. Kuma, A.; Hatano, M.; Matsui, M.; Yamamoto, A., The role of autophagy during the early neonatal starvation period. *Nature* **2004**, 432, 1032.

15. Amaravadi, R. K.; Lippincott-Schwartz, J.; Yin, X.-M.; Weiss, W. A.; Takebe, N.; Timmer, W.; DiPaola, R.

S.; Lotze, M. T.; White, E., Principles and current strategies for targeting autophagy for cancer treatment. *Clinical cancer research* **2011**, 17, 654-666.

16. Kondo, Y.; Kanzawa, T.; Sawaya, R.; Kondo, S., The role of autophagy in cancer development and response to therapy. *Nature Reviews Cancer* **2005**, 5, 726-734.

17. Chen, S.; Rehman, S. K.; Zhang, W.; Wen, A.; Yao, L.; Zhang, J., Autophagy is a therapeutic target in anticancer drug resistance. *Biochimica et Biophysica Acta (BBA)-Reviews on Cancer* **2010**, 1806, 220-229.

18. Mohammad, R. M.; Muqbil, I.; Lowe, L.; Yedjou, C.; Hsu, H.-Y.; Lin, L.-T.; Siegelin, M. D.; Fimognari, C.; Kumar, N. B.; Dou, Q. P. Broad targeting of resistance to apoptosis in cancer. In Seminars in cancer biology, 2015; Elsevier: 2015; Vol. 35; pp S78-S103.

19. Fan, Q.-W.; Cheng, C.; Hackett, C.; Feldman, M.; Houseman, B. T.; Nicolaides, T.; Haas-Kogan, D.; James, C. D.; Oakes, S. A.; Debnath, J., Akt and autophagy cooperate to promote survival of drug-resistant glioma. *Science signaling* **2010**, 3, ra81.

20. Rodon, J.; Dienstmann, R.; Serra, V.; Tabernero, J., Development of PI3K inhibitors: lessons learned from early clinical trials. *Nature reviews Clinical oncology* **2013**, 10, 143-153.

21. Cortes, C. J.; Qin, K.; Cook, J.; Solanki, A.; Mastrianni, J. A., Rapamycin delays disease onset and prevents PrP plaque deposition in a mouse model of Gerstmann–Sträussler–Scheinker disease. *Journal of Neuroscience* **2012**, 32, 12396-12405.

22. Jiang, T.-F.; Zhang, Y.-J.; Zhou, H.-Y.; Wang, H.-M.; Tian, L.-P.; Liu, J.; Ding, J.-Q.; Chen, S.-D.,

Curcumin ameliorates the neurodegenerative pathology in A53T α-synuclein cell model of Parkinson's disease through the downregulation of mTOR/p70S6K signaling and the recovery of macroautophagy. *Journal of NeuroImmune Pharmacology* **2013**, 8, 356-369.

23. Wu, Y.; Li, X.; Zhu, J. X.; Xie, W.; Le, W.; Fan, Z.; Jankovic, J.; Pan, T., Resveratrol-activated AMPK/SIRT1/autophagy in cellular models of Parkinson's disease. *Neurosignals* **2011**, 19, 163-174.

24. Sharma, S.; Yao, H.-P.; Zhou, Y.-Q.; Zhou, J.; Zhang, R.; Wang, M.-H., Prevention of BMS‐777607‐induced polyploidy/senescence by mTOR inhibitor AZD8055 sensitizes breast cancer cells to cytotoxic chemotherapeutics. *Molecular oncology* **2014**, 8, 469-482.

25. Engelman, J. A.; Chen, L.; Tan, X.; Crosby, K.; Guimaraes, A. R.; Upadhyay, R.; Maira, M.; McNamara, K.; Perera, S. A.; Song, Y., Effective use of PI3K and MEK inhibitors to treat mutant Kras G12D and PIK3CA H1047R murine lung cancers. *Nature medicine* **2008**, 14, 1351-1356.

26. Markman, B.; Tabernero, J.; Krop, I.; Shapiro, G.; Siu, L.; Chen, L.; Mita, M.; Cuero, M. M.; Stutvoet, S.; Birle, D., Phase I safety, pharmacokinetic, and pharmacodynamic study of the oral phosphatidylinositol-3-kinase and mTOR inhibitor BGT226 in patients with advanced solid tumors. *Annals of Oncology* **2012**, 23, 2399-2408.

27. Wen, P. Y.; Omuro, A.; Ahluwalia, M. S.; Fathallah-Shaykh, H. M.; Mohile, N.; Lager, J. J.; Laird, A. D.; Tang, J.; Jiang, J.; Egile, C., Phase I dose-escalation study of the PI3K/mTOR inhibitor voxtalisib (SAR245409, XL765) plus temozolomide with or without radiotherapy in patients with high-grade glioma. *Neuro-oncology* **2015**, nov083.

28. Stern, H. M.; Kutok, J. L., In; Google Patents: 2013.

29. Hsu, K.; Lager, J.; Ogden, J., In; Google Patents: 2014.

30. Ihle, N. T.; Lemos, R.; Wipf, P.; Yacoub, A.; Mitchell, C.; Siwak, D.; Mills, G. B.; Dent, P.; Kirkpatrick, D. L.; Powis, G., Mutations in the phosphatidylinositol-3-kinase pathway predict for antitumor activity of the inhibitor PX-866 whereas oncogenic Ras is a dominant predictor for resistance. *Cancer research* **2009**, 69, 143-150.

31. Munugalavadla, V.; Mariathasan, S.; Slaga, D.; Du, C.; Berry, L.; Del Rosario, G.; Yan, Y.; Boe, M.; Sun, L.; Friedman, L., The PI3K inhibitor GDC-0941 combines with existing clinical regimens for superior activity in multiple myeloma. *Oncogene* **2014**, 33, 316-325.

32. Brachmann, S. M.; Kleylein-Sohn, J.; Gaulis, S.; Kauffmann, A.; Blommers, M. J.; Kazic-Legueux, M.; Laborde, L.; Hattenberger, M.; Stauffer, F.; Vaxelaire, J., Characterization of the mechanism of action of the pan class I PI3K inhibitor NVP-BKM120 across a broad range of concentrations. *Molecular cancer therapeutics* **2012**, 11, 1747-1757.

33. Jin, F.; Robeson, M.; Zhou, H.; Moyer, C.; Wilbert, S.; Murray, B.; Ramanathan, S., Clinical drug interaction profile of idelalisib in healthy subjects. *The Journal of Clinical Pharmacology* **2015**, 55, 909-919.

34. Kondapaka, S. B.; Singh, S. S.; Dasmahapatra, G. P.; Sausville, E. A.; Roy, K. K., Perifosine, a novel alkylphospholipid, inhibits protein kinase B activation. *Molecular Cancer Therapeutics* **2003**, 2, 1093-1103.

35. Rhodes, N.; Heerding, D. A.; Duckett, D. R.; Eberwein, D. J.; Knick, V. B.; Lansing, T. J.; McConnell, R. T.; Gilmer, T. M.; Zhang, S.-Y.; Robell, K., Characterization of an Akt kinase inhibitor with potent pharmacodynamic and antitumor activity. *Cancer research* **2008**, 68, 2366-2374.

36. Gürsel, D. B.; Connell-Albert, Y. S.; Tuskan, R. G.; Anastassiadis, T.; Walrath, J. C.; Hawes, J. J.; Amlin-Van Schaick, J. C.; Reilly, K. M., Control of proliferation in astrocytoma cells by the receptor tyrosine kinase/PI3K/AKT signaling axis and the use of PI-103 and TCN as potential anti-astrocytoma therapies. *Neuro-oncology* **2011**, 13, 610-621.

37. Lin, Y.-H.; Chen, B. Y.-H.; Lai, W.-T.; Wu, S.-F.; Guh, J.-H.; Cheng, A.-L.; Hsu, L.-C., The Akt inhibitor MK-2206 enhances the cytotoxicity of paclitaxel (Taxol) and cisplatin in ovarian cancer cells. *Naunyn-Schmiedeberg's archives of pharmacology* **2015**, 388, 19-31.

38. Ma, T. C.; Buescher, J. L.; Oatis, B.; Funk, J. A.; Nash, A. J.; Carrier, R. L.; Hoyt, K. R., Metformin therapy in a transgenic mouse model of Huntington's disease. *Neuroscience letters* **2007**, 411, 98-103.

39. Lan, D.-M.; Liu, F.-T.; Zhao, J.; Chen, Y.; Wu, J.-J.; Ding, Z.-T.; Yue, Z.-Y.; Ren, H.-M.; Jiang, Y.-P.; Wang, J., Effect of trehalose on PC12 cells overexpressing wild-type or A53T mutant α-synuclein. *Neurochemical research* **2012**, 37, 2025-2032.

40. Rose, C.; Menzies, F. M.; Renna, M.; Acevedo-Arozena, A.; Corrochano, S.; Sadiq, O.; Brown, S. D.; Rubinsztein, D. C., Rilmenidine attenuates toxicity of polyglutamine expansions in a mouse model of Huntington's disease. *Human molecular genetics* **2010**, 19, 2144-2153.

41. Carew, J. S.; Nawrocki, S. T.; Kahue, C. N.; Zhang, H.; Yang, C.; Chung, L.; Houghton, J. A.; Huang, P.;

Giles, F. J.; Cleveland, J. L., Targeting autophagy augments the anticancer activity of the histone deacetylase inhibitor SAHA to overcome Bcr-Abl–mediated drug resistance. *Blood* **2007**, 110, 313-322.

42. Boya, P.; González-Polo, R.-A.; Casares, N.; Perfettini, J.-L.; Dessen, P.; Larochette, N.; Métivier, D.; Meley, D.; Souquere, S.; Yoshimori, T., Inhibition of macroautophagy triggers apoptosis. *Molecular and cellular biology* **2005**, 25, 1025-1040.

43. Wu, D.; Qiu, T.; Zhang, Q.; Kang, H.; Yuan, S.; Zhu, L.; Zhu, R., Systematic toxicity mechanism analysis of proton pump inhibitors: an in silico study. *Chemical research in toxicology* **2015**, 28, 419-430.

44. Spence, S.; Deurinck, M.; Ju, H.; Traebert, M.; McLean, L.; Marlowe, J.; Emotte, C.; Tritto, E.; Tseng, M.; Shultz, M., Histone deacetylase inhibitors prolong cardiac repolarization through transcriptional mechanisms. *Toxicological Sciences* **2016**, 153, 39-54.

45. Athar, M.; Back, J. H.; Tang, X.; Kim, K. H.; Kopelovich, L.; Bickers, D. R.; Kim, A. L., Resveratrol: a review of preclinical studies for human cancer prevention. *Toxicology and applied pharmacology* **2007**, 224, 274-283.

46. Fisher, B.; Costantino, J. P.; Wickerham, D. L.; Redmond, C. K.; Kavanah, M.; Cronin, W. M.; Vogel, V.; Robidoux, A.; Dimitrov, N.; Atkins, J., Tamoxifen for prevention of breast cancer: report of the National Surgical Adjuvant Breast and Bowel Project P-1 Study. *Journal of the National Cancer Institute* **1998**, 90, 1371-1388.

47. Williams, A.; Sarkar, S.; Cuddon, P.; Ttofi, E. K.; Saiki, S.; Siddiqi, F. H.; Jahreiss, L.; Fleming, A.; Pask, D.; Goldsmith, P., Novel targets for Huntington's disease in an mTOR-independent autophagy pathway.

Nature chemical biology **2008**, 4, 295-305.

48. Li, L.; Zhang, S.; Zhang, X.; Li, T.; Tang, Y.; Liu, H.; Yang, W.; Le, W., Autophagy enhancer carbamazepine alleviates memory deficits and cerebral amyloid-β pathology in a mouse model of Alzheimer's disease. *Current Alzheimer Research* **2013**, 10, 433-441.

49. Sarkar, S.; Ravikumar, B.; Floto, R.; Rubinsztein, D., Rapamycin and mTOR-independent autophagy inducers ameliorate toxicity of polyglutamine-expanded huntingtin and related proteinopathies. *Cell Death & Differentiation* **2009**, 16, 46-56.

50. Engelman, J. A., Targeting PI3K signalling in cancer: opportunities, challenges and limitations. *Nature Reviews Cancer* **2009**, 9, 550-562.

51. Choo, A. Y.; Blenis, J., Not all substrates are treated equally: Implications for mTOR, rapamycin-resistance, and cancer therapy. *Cell Cycle* **2009**, 8, 567-572.

52. Feldman, M. E.; Apsel, B.; Uotila, A.; Loewith, R.; Knight, Z. A.; Ruggero, D.; Shokat, K. M., Active-site inhibitors of mTOR target rapamycin-resistant outputs of mTORC1 and mTORC2. *PLoS Biol* **2009**, 7, e1000038.

53. Guha, S.; Baltazar, G. C.; Tu, L. A.; Liu, J.; Lim, J. C.; Lu, W.; Argall, A.; Boesze‐Battaglia, K.; Laties, A. M.; Mitchell, C. H., Stimulation of the D5 dopamine receptor acidifies the lysosomal pH of retinal pigmented epithelial cells and decreases accumulation of autofluorescent photoreceptor debris. *Journal of neurochemistry* **2012**, 122, 823-833.

54. Finbloom, D.; Silver, K.; Newsome, D.; Gunkel, R., Comparison of hydroxychloroquine and chloroquine

use and the development of retinal toxicity. *The Journal of rheumatology* **1985**, 12, 692-694.

55. Maday, S.; Wallace, K. E.; Holzbaur, E. L., Autophagosomes initiate distally and mature during transport toward the cell soma in primary neurons. *J Cell Biol* **2012**, 196, 407-417.

56. Levine, B.; Kroemer, G., Autophagy in aging, disease and death: the true identity of a cell death impostor. *Cell Death Differ.* **2009**, 16, 1-2.

57. Komatsu, M.; Waguri, S.; Chiba, T.; Murata, S.; Iwata, J.-i.; Tanida, I.; Ueno, T.; Koike, M.; Uchiyama, Y.; Kominami, E., Loss of autophagy in the central nervous system causes neurodegeneration in mice. *Nature* **2006**, 441, 880-884.

58. Martinez-Vicente, M.; Sovak, G.; Cuervo, A. M., Protein degradation and aging. *Experimental gerontology* **2005**, 40, 622-633.

59. Nixon, R. A., The role of autophagy in neurodegenerative disease. *Nature medicine* **2013**, 19, 983-997.

60. Koike, M.; Shibata, M.; Tadakoshi, M.; Gotoh, K.; Komatsu, M.; Waguri, S.; Kawahara, N.; Kuida, K.; Nagata, S.; Kominami, E., Inhibition of autophagy prevents hippocampal pyramidal neuron death after hypoxic-ischemic injury. *The American journal of pathology* **2008**, 172, 454-469.

61. Li, Q.; Liu, Y.; Sun, M., Autophagy and Alzheimer's Disease. *Cell Mol Neurobiol.* **2016**.

62. Nixon, R. A.; Wegiel, J.; Kumar, A.; Yu, W. H.; Peterhoff, C.; Cataldo, A.; Cuervo, A. M., Extensive involvement of autophagy in Alzheimer disease: an immuno-electron microscopy study. *Journal of Neuropathology & Experimental Neurology* **2005**, 64, 113-122.

63. Sanchez-Varo, R.; Trujillo-Estrada, L.; Sanchez-Mejias, E.; Torres, M.; Baglietto-Vargas, D.; Moreno-Gonzalez, I.; De Castro, V.; Jimenez, S.; Ruano, D.; Vizuete, M., Abnormal accumulation of autophagic vesicles correlates with axonal and synaptic pathology in young Alzheimer's mice hippocampus. *Acta neuropathologica* **2012**, 123, 53-70.

64. Wolfe, D. M.; Lee, J. h.; Kumar, A.; Lee, S.; Orenstein, S. J.; Nixon, R. A., Autophagy failure in Alzheimer's disease and the role of defective lysosomal acidification. *European Journal of Neuroscience* **2013**, 37, 1949-1961.

65. Ji, Z.-S.; Müllendorff, K.; Cheng, I. H.; Miranda, R. D.; Huang, Y.; Mahley, R. W., Reactivity of apolipoprotein E4 and amyloid β peptide lysosomal stability and neurodegeneration. *Journal of Biological Chemistry* **2006**, 281, 2683-2692.

66. Zhou, F.; van Laar, T.; Huang, H.; Zhang, L., APP and APLP1 are degraded through autophagy in response to proteasome inhibition in neuronal cells. *Protein & cell* **2011**, 2, 377-383.

67. Son, S. M.; Jung, E. S.; Shin, H. J.; Byun, J.; Mook-Jung, I., Aβ-induced formation of autophagosomes is mediated by RAGE-CaMKKβ-AMPK signaling. *Neurobiology of aging* **2012**, 33, 1006. e11-1006. e23.

68. Yu, W. H.; Cuervo, A. M.; Kumar, A.; Peterhoff, C. M.; Schmidt, S. D.; Lee, J.-H.; Mohan, P. S.; Mercken, M.; Farmery, M. R.; Tjernberg, L. O., Macroautophagy—a novel β-amyloid peptide-generating pathway activated in Alzheimer's disease. *J Cell Biol* **2005**, 171, 87-98.

69. Congdon, E. E.; Wu, J. W.; Myeku, N.; Figueroa, Y. H.; Herman, M.; Marinec, P. S.; Gestwicki, J. E.; Dickey, C. A.; Yu, W. H.; Duff, K. E., Methylthioninium chloride (methylene blue) induces autophagy and

attenuates tauopathy in vitro and in vivo. *Autophagy* **2012**, 8, 609-622.

70. Singleton, A.; Farrer, M.; Johnson, J.; Singleton, A.; Hague, S.; Kachergus, J.; Hulihan, M.; Peuralinna, T.; Dutra, A.; Nussbaum, R., α-Synuclein locus triplication causes Parkinson's disease. *Science* **2003**, 302, 841-841.

71. Yu, W. H.; Dorado, B.; Figueroa, H. Y.; Wang, L.; Planel, E.; Cookson, M. R.; Clark, L. N.; Duff, K. E., Metabolic activity determines efficacy of macroautophagic clearance of pathological oligomeric α-synuclein. *The American journal of pathology* **2009**, 175, 736-747.

72. Webb, J. L.; Ravikumar, B.; Atkins, J.; Skepper, J. N.; Rubinsztein, D. C., α-Synuclein is degraded by both autophagy and the proteasome. *Journal of Biological Chemistry* **2003**, 278, 25009-25013.

73. AR, W., Impairs macroautophagy: implications for Parkinson's disease. *J Cell Biol* **2010**, 190, 1023-37.

74. Lewy, F., Paralysis agitans. I. Pathologische Anatomie Ed. *M Lewandowski.* **1912**, 920-33.

75. Sarkar, S.; Rubinsztein, D. C., Huntington's disease: degradation of mutant huntingtin by autophagy. *FEBS journal* **2008**, 275, 4263-4270.

76. Caccamo, A.; Majumder, S.; Richardson, A.; Strong, R.; Oddo, S., Molecular interplay between mammalian target of rapamycin (mTOR), amyloid-β, and tau effects on cognitive impairments. *Journal of Biological Chemistry* **2010**, 285, 13107-13120.

77. Sarkar, S.; Davies, J. E.; Huang, Z.; Tunnacliffe, A.; Rubinsztein, D. C., Trehalose, a novel mTOR-independent autophagy enhancer, accelerates the clearance of mutant huntingtin and α-synuclein. *Journal of Biological Chemistry* **2007**, 282, 5641-5652.

78. Feng, H.-L.; Leng, Y.; Ma, C.-H.; Zhang, J.; Ren, M.; Chuang, D.-M., Combined lithium and valproate treatment delays disease onset, reduces neurological deficits and prolongs survival in an amyotrophic lateral sclerosis mouse model. *Neuroscience* **2008**, 155, 567-572.

79. Jeong, H.; Then, F.; Melia, T. J.; Mazzulli, J. R.; Cui, L.; Savas, J. N.; Voisine, C.; Paganetti, P.; Tanese, N.; Hart, A. C., Acetylation targets mutant huntingtin to autophagosomes for degradation. *Cell* **2009**, 137, 60-72.

80. Lee, J.-A.; Gao, F.-B., Inhibition of autophagy induction delays neuronal cell loss caused by dysfunctional ESCRT-III in frontotemporal dementia. *Journal of Neuroscience* **2009**, 29, 8506-8511.

81. Wong, R. S., Apoptosis in cancer: from pathogenesis to treatment. *Journal of Experimental & Clinical Cancer Research* **2011**, 30, 87.

82. Jean, Y., Nucleo-cytoplasmic communication in apoptotic response to genotoxic and inflammatory stress. *Cell research* **2005**, 15, 43-48.

83. Igney, F. H. e. a., Death and anti-death: Tumor resistance to apoptosis. *Nat Rev. Cancer.* **2002**, 2, 277-88.

84. Bai, L.; Wang, S., Targeting apoptosis pathways for new cancer therapeutics. *Annual review of medicine* **2014**, 65, 139-155.

85. Roberts, A. W.; Davids, M. S.; Pagel, J. M.; Kahl, B. S.; Puvvada, S. D.; Gerecitano, J. F.; Kipps, T. J.; Anderson, M. A.; Brown, J. R.; Gressick, L., Targeting BCL2 with venetoclax in relapsed chronic lymphocytic leukemia. *New England Journal of Medicine* **2016**, 374, 311-322.

86. Wilson, W. H.; O'Connor, O. A.; Czuczman, M. S.; LaCasce, A. S.; Gerecitano, J. F.; Leonard, J. P.;

Tulpule, A.; Dunleavy, K.; Xiong, H.; Chiu, Y.-L., Navitoclax, a targeted high-affinity inhibitor of BCL-2, in lymphoid malignancies: a phase 1 dose-escalation study of safety, pharmacokinetics, pharmacodynamics, and antitumour activity. *The lancet oncology* **2010**, 11, 1149-1159.

87. Nguyen, M.; Marcellus, R. C.; Roulston, A.; Watson, M.; Serfass, L.; Madiraju, S. M.; Goulet, D.; Viallet, J.; Bélec, L.; Billot, X., Small molecule obatoclax (GX15-070) antagonizes MCL-1 and overcomes MCL-1-mediated resistance to apoptosis. *Proceedings of the National Academy of Sciences* **2007**, 104, 19512-19517.

88. Balakrishnan, K.; Wierda, W. G.; Keating, M. J.; Gandhi, V., Gossypol, a BH3 mimetic, induces apoptosis in chronic lymphocytic leukemia cells. *Blood* **2008**, 112, 1971-1980.

89. Wu, Y.; Kazumura, K.; Maruyama, W.; Osawa, T.; Naoi, M., Rasagiline and selegiline suppress calcium efflux from mitochondria by PK11195-induced opening of mitochondrial permeability transition pore: a novel anti-apoptotic function for neuroprotection. *Journal of Neural Transmission* **2015**, 122, 1399-1407.

90. Tchoghandjian, A.; Soubéran, A.; Tabouret, E.; Colin, C.; Denicolaï, E.; Jiguet-Jiglaire, C.; El-Battari, A.; Villard, C.; Baeza-Kallee, N.; Figarella-Branger, D., Inhibitor of apoptosis protein expression in glioblastomas and their in vitro and in vivo targeting by SMAC mimetic GDC-0152. *Cell Death & Disease* **2016**, 7, e2325.

91. Tolcher, A. W.; Bendell, J. C.; Papadopoulos, K. P.; Burris, H. A.; Patnaik, A.; Fairbrother, W. J.; Wong, H.; Budha, N.; Darbonne, W. C.; Peale, F., A Phase I Dose-Escalation Study Evaluating the Safety Tolerability and Pharmacokinetics of CUDC-427, a Potent, Oral, Monovalent IAP Antagonist, in Patients with Refractory Solid Tumors. *Clinical Cancer Research* **2016**, 22, 4567-4573.

92. Srivastava, A. K.; Jaganathan, S.; Stephen, L.; Hollingshead, M. G.; Layhee, A.; Damour, E.; Govindharajulu, J. P.; Donohue, J.; Esposito, D.; Mapes, J. P., Effect of a Smac mimetic (TL32711, Birinapant) on the apoptotic program and apoptosis biomarkers examined with validated multiplex immunoassays fit for clinical use. *Clinical Cancer Research* **2016**, 22, 1000-1010.

93. Infante, J. R.; Dees, E. C.; Olszanski, A. J.; Dhuria, S. V.; Sen, S.; Cameron, S.; Cohen, R. B., Phase I dose-escalation study of LCL161, an oral inhibitor of apoptosis proteins inhibitor, in patients with advanced solid tumors. *Journal of Clinical Oncology* **2014**, 32, 3103-3110.

94. DiPersio, J. F.; Erba, H. P.; Larson, R. A.; Luger, S. M.; Tallman, M. S.; Brill, J. M.; Vuagniaux, G.; Rouits, E.; Sorensen, J. M.; Zanna, C., Oral Debio1143 (AT406), an antagonist of inhibitor of apoptosis proteins, combined with daunorubicin and cytarabine in patients with poor-risk acute myeloid leukemia—results of a phase I dose-escalation study. *Clinical Lymphoma Myeloma and Leukemia* **2015**, 15, 443-449.

95. Tovar, C.; Graves, B.; Packman, K.; Filipovic, Z.; Xia, B. H. M.; Tardell, C.; Garrido, R.; Lee, E.; Kolinsky, K.; To, K.-H., MDM2 small-molecule antagonist RG7112 activates p53 signaling and regresses human tumors in preclinical cancer models. *Cancer research* **2013**, 73, 2587-2597.

96. Townsend, E. C.; DeSouza, T.; Murakami, M. A.; Montero, J.; Stevenson, K.; Christie, A. L.; Christodolou, A. N.; Vojinovic, U.; Kopp, N.; Barzaghi-Rinaudo, P., The MDM2 Inhibitor NVP-CGM097 Is highly active in a randomized preclinical trial of B-cell acute lymphoblastic leukemia patient derived xenografts. *Blood* **2015**, 126, 797-797.

97. Li, J.; Chen, J.; Mo, H.; Chen, J.; Qian, C.; Yan, F.; Gu, C.; Hu, Q.; Wang, L.; Chen, G., Minocycline

protects against NLRP3 inflammasome-induced inflammation and P53-associated apoptosis in early brain injury after subarachnoid hemorrhage. *Molecular neurobiology* **2016**, 53, 2668-2678.

98. Ghavami, S.; Shojaei, S.; Yeganeh, B.; Ande, S. R.; Jangamreddy, J. R.; Mehrpour, M.; Christoffersson, J.; Chaabane, W.; Moghadam, A. R.; Kashani, H. H., Autophagy and apoptosis dysfunction in neurodegenerative disorders. *Progress in neurobiology* **2014**, 112, 24-49.

99. Lustbader, J. W.; Cirilli, M.; Lin, C.; Xu, H. W.; Takuma, K.; Wang, N.; Caspersen, C.; Chen, X.; Pollak, S.; Chaney, M., ABAD directly links Aß to mitochondrial toxicity in Alzheimer's Disease. *Science* **2004**, 304, 448-452.

100. Loo, D. T.; Copani, A.; Pike, C. J.; Whittemore, E. R.; Walencewicz, A. J.; Cotman, C. W., Apoptosis is induced by beta-amyloid in cultured central nervous system neurons. *Proceedings of the National Academy of Sciences* **1993**, 90, 7951-7955.

101. Kountouras, J.; Zavos, C.; Polyzos, S.; Deretzi, G.; Vardaka, E.; Giartza‐Taxidou, E.; Katsinelos, P.; Rapti, E.; Chatzopoulos, D.; Tzilves, D., Helicobacter pylori infection and Parkinson's disease: apoptosis as an underlying common contributor. *European journal of neurology* **2012**, 19, e56-e56.

102. Fitzwalter, B. E.; Thorburn, A., Recent insights into cell death and autophagy. *FEBS journal* **2015**, 282, 4279-4288.

103. Liu, H.; Wang, L.; Lv, M.; Pei, R.; Li, P.; Pei, Z.; Wang, Y.; Su, W.; Xie, X.-Q., AlzPlatform: an Alzheimer's disease domain-specific chemogenomics knowledgebase for polypharmacology and target identification research. *Journal of chemical information and modeling* **2014**, 54, 1050-1060.

104. Xu, X.; Ma, S.; Feng, Z.; Hu, G.; Wang, L.; Xie, X.-Q., Chemogenomics knowledgebase and systems pharmacology for hallucinogen target identification—Salvinorin A as a case study. *Journal of Molecular Graphics and Modelling* **2016**, 70, 284-295.

105. Trott, O.; Olson, A. J., AutoDock Vina: improving the speed and accuracy of docking with a new scoring function, efficient optimization, and multithreading. *J Comput Chem* **2010**, 31, 455-61.

106. Wang, L.; Ma, C.; Wipf, P.; Liu, H.; Su, W.; Xie, X.-Q., TargetHunter: an in silico target identification tool for predicting therapeutic potential of small organic molecules based on chemogenomic database. *The AAPS journal* **2013**, 15, 395-406.

107. Xie, X. Q.; Chen, J. Z.; Billings, E. M., 3D structural model of the G‐protein‐coupled cannabinoid CB2 receptor. *Proteins: Structure, Function, and Bioinformatics* **2003**, 53, 307-319.

108. Vapnik, V. N., *The nature of statistical learning theory*. Springer: New York, 1995.

109. Zhao, Y. H.; Abraham, M. H.; Ibrahim, A.; Fish, P. V.; Cole, S.; Lewis, M. L.; de Groot, M. J.; Reynolds, D. P., Predicting penetration across the blood-brain barrier from simple descriptors and fragmentation schemes. *Journal of chemical information and modeling* **2007**, 47, 170-175.

110. Rosner, B. Two-Sample t Test for Independent Samples with Unequal Variance. In *Fundamentals of Biostatistics (7th Edition)*; Cengage Learning: Boston, MA, 2010, pp 287-293.

111. Rosner, B. The Wilcoxon Rank-Sum Test. In *Fundamentals of Biostatistics (7th Edition)*; Cengage Learning: Boston, MA, 2010; Chapter 339-344.

112. Olivier, B.; Rohwer, J.; Hofmeyr, J.-H., Modelling cellular processes with Python and Scipy. *Molecular*

biology reports **2002**, 29, 249-254.

113. Balius, T. E.; Mukherjee, S.; Rizzo, R. C., Implementation and evaluation of a docking ‐ rescoring method using molecular footprint comparisons. *Journal of computational chemistry* **2011**, 32, 2273-2289.

114. Ruxton, G. D., The unequal variance t-test is an underused alternative to Student's t-test and the Mann–Whitney U test. *Behavioral Ecology* **2006**, 17, 688-690.

115. d'Agostino, R. B., An omnibus test of normality for moderate and large size samples. *Biometrika* **1971**, 341-348.

116. Curtin, F.; Schulz, P., Multiple correlations and Bonferroni's correction. *Biological psychiatry* **1998**, 44, 775-777.

117. Fawcett, T., An introduction to ROC analysis. *Pattern recognition letters* **2006**, 27, 861-874.

118. Nagashima, K.; Shumway, S. D.; Sathyanarayanan, S.; Chen, A. H.; Dolinski, B.; Xu, Y.; Keilhack, H.; Nguyen, T.; Wiznerowicz, M.; Li, L., Genetic and pharmacological inhibition of PDK1 in cancer cells characterization of a selective allosteric kinase inhibitor. *Journal of Biological Chemistry* **2011**, 286, 6433-6448.

119. Zhao, Y.; Zhang, X.; Chen, Y.; Lu, S.; Peng, Y.; Wang, X.; Guo, C.; Zhou, A.; Zhang, J.; Luo, Y., Crystal structures of PI3Kα complexed with PI103 and its derivatives: new directions for inhibitors design. *ACS medicinal chemistry letters* **2013**, 5, 138-142.

120. McHardy, T.; Caldwell, J. J.; Cheung, K.-M.; Hunter, L. J.; Taylor, K.; Rowlands, M.; Ruddle, R.; Henley, A.; de Haven Brandon, A.; Valenti, M., Discovery of 4-amino-1-(7 H-pyrrolo [2, 3-d] pyrimidin-4-yl)

piperidine-4-carboxamides as selective, orally active inhibitors of protein kinase B (Akt). *Journal of medicinal chemistry* **2010**, 53, 2239-2249.

121. Huang, X.; Begley, M.; Morgenstern, K. A.; Gu, Y.; Rose, P.; Zhao, H.; Zhu, X., Crystal structure of an inactive Akt2 kinase domain. *Structure* **2003**, 11, 21-30.

122. Follis, A. V.; Chipuk, J. E.; Fisher, J. C.; Yun, M.-K.; Grace, C. R.; Nourse, A.; Baran, K.; Ou, L.; Min, L.; White, S. W., PUMA binding induces partial unfolding within BCL-xL to disrupt p53 binding and promote apoptosis. *Nature chemical biology* **2013**, 9, 163-168.

123. Mizushima, N.; Levine, B.; Cuervo, A. M.; Klionsky, D. J., Autophagy fights disease through cellular self-digestion. *Nature* **2008**, 451, 1069-1075.

124. Hwang, S. H.; Wecksler, A. T.; Zhang, G.; Morisseau, C.; Nguyen, L. V.; Fu, S. H.; Hammock, B. D., Synthesis and biological evaluation of sorafenib-and regorafenib-like sEH inhibitors. *Bioorganic & medicinal chemistry letters* **2013**, 23, 3732-3737.

125. Erickson, J. A.; Jalaie, M.; Robertson, D. H.; Lewis, R. A.; Vieth, M., Lessons in molecular recognition: the effects of ligand and protein flexibility on molecular docking accuracy. *Journal of medicinal chemistry* **2004**, 47, 45-55.

126. Marsilje, T. H.; Pei, W.; Chen, B.; Lu, W.; Uno, T.; Jin, Y.; Jiang, T.; Kim, S.; Li, N.; Warmuth, M., Synthesis, structure–activity relationships, and in vivo efficacy of the novel potent and selective anaplastic lymphoma kinase (ALK) inhibitor 5-Chloro-N 2-(2-isopropoxy-5-methyl-4-(piperidin-4-yl) phenyl)-N 4-(2-(isopropylsulfonyl) phenyl) pyrimidine-2, 4-diamine (LDK378) currently in phase 1 and phase 2

clinical trials. *Journal of medicinal chemistry* **2013**, 56, 5675-5690.

127. Cui, J. J.; Tran-Dubé, M.; Shen, H.; Nambu, M.; Kung, P.-P.; Pairish, M.; Jia, L.; Meng, J.; Funk, L.; Botrous, I., Structure based drug design of crizotinib (PF-02341066), a potent and selective dual inhibitor of mesenchymal–epithelial transition factor (c-MET) kinase and anaplastic lymphoma kinase (ALK). *Journal of medicinal chemistry* **2011**, 54, 6342-6363.

128. Mahboobi, S.; Sellmer, A.; Winkler, M.; Eichhorn, E.; Pongratz, H.; Ciossek, T.; Baer, T.; Maier, T.; Beckers, T., Novel chimeric histone deacetylase inhibitors: a series of lapatinib hybrides as potent inhibitors of epidermal growth factor receptor (EGFR), human epidermal growth factor receptor 2 (HER2), and histone deacetylase activity. *Journal of medicinal chemistry* **2010**, 53, 8546-8555.

129. Finlay, M. R. V.; Anderton, M.; Ashton, S.; Ballard, P.; Bethel, P. A.; Box, M. R.; Bradbury, R. H.; Brown, S. J.; Butterworth, S.; Campbell, A., In; ACS Publications: 2014.

130. Apsel, B.; Blair, J. A.; Gonzalez, B.; Nazif, T. M.; Feldman, M. E.; Aizenstein, B.; Hoffman, R.; Williams, R. L.; Shokat, K. M.; Knight, Z. A., Targeted polypharmacology: discovery of dual inhibitors of tyrosine and phosphoinositide kinases. *Nature chemical biology* **2008**, 4, 691-699.

131. Pandey, U. B.; Nie, Z.; Batlevi, Y.; McCray, B. A.; Ritson, G. P.; Nedelsky, N. B.; Schwartz, S. L.; DiProspero, N. A.; Knight, M. A.; Schuldiner, O., HDAC6 rescues neurodegeneration and provides an essential link between autophagy and the UPS. *Nature* **2007**, 447, 860-864.

132. Lee, J. Y.; Koga, H.; Kawaguchi, Y.; Tang, W.; Wong, E.; Gao, Y. S.; Pandey, U. B.; Kaushik, S.; Tresse, E.; Lu, J., HDAC6 controls autophagosome maturation essential for ubiquitin–selective quality–control

autophagy. *The EMBO journal* **2010**, 29, 969-980.

133. Jones, P.; Altamura, S.; De Francesco, R.; Gallinari, P.; Lahm, A.; Neddermann, P.; Rowley, M.; Serafini, S.; Steinkühler, C., Probing the elusive catalytic activity of vertebrate class IIa histone deacetylases. *Bioorganic & medicinal chemistry letters* **2008**, 18, 1814-1819.

134. Fredenhagen, A.; Kittelmann, M.; Oberer, L.; Kuhn, A.; Kühnöl, J.; Délémonté, T.; Aichholz, R.; Wang, P.; Atadja, P.; Shultz, M. D., Biocatalytic synthesis and structure elucidation of cyclized metabolites of the deacetylase inhibitor panobinostat (LBH589). *Drug Metabolism and Disposition* **2012**, 40, 1041-1050.

135. Miller, T. A.; Witter, D. J.; Belvedere, S., Histone deacetylase inhibitors. *Journal of medicinal chemistry* **2003**, 46, 5097-5116.

136. Doctor, K.; Reed, J.; Godzik, A.; Bourne, P., The apoptosis database. *Cell Death & Differentiation* **2003**, 10, 621-633.